UNIVERSITÀ POLITECNICA DELLE MARCHE
FACOLTÀ DI INGEGNERIA

Corso di Laurea Magistrale in Biomedical Engineering

Myoelectric Based Identification of Handwritten Words: A Pattern Recognition Approach

Relatore:
Ing. Alessandro Mengarelli

Tesi di Laurea di:
Federica Cerritelli

Correlatori:
Prof. Sandro Fioretti
Ing. Andrea Tigrini

A.A. 2021/2022

Acknowledgements

I would like to strongly thank my Supervisor Alessandro Mengarelli, my co-Supervisors Sandro Fioretti and Andrea Tigrini, and the Professor Federica Verdini for helping me constantly in this work, from the first research to the final observation of the results and for reviewing this manuscript.

I would also like to thank all my friends and my roommates, Roberta Sorressa, for always being there for me like a sister, and my special colleague and dearest friend Valeria Scolastra, who accompanied me through our study course. And thanks to you, Riccardo Cavallo, for your ability to always make me smile.

Special thanks to my family and to Mom and Dad, for giving me the chance to enrol in this course and for always believing in me throughout my entire life.

Contents

Abstract

Introduction. The purpose of this thesis is to provide a reliable classification model that can accurately distinguish between 30 different handwritten words, using only the information contained in the forearm and wrist muscles activations, that occur when a particular handwriting task is performed. Along with this major objective, also some factors that are critical for building a strong handwritten character classification model are investigated. Firstly, it was investigated the most appropriate electrodes' setup for the specific EMG pattern recognition. Furthermore, considering that the way to access myoelectric information content is through the feature extraction, a careful selection of them is performed, considering some of the most used feature sets available in literature, to find which has the best information content.

Materials and methods. Six healthy subjects were asked to write 30 words, each one repeated 10 times, with a pen on the paper with their natural way of writing in cursive. The electrodes setup is defined with 6 EMG electrodes, 4 placed on the forearm and 2 on the wrist. After the EMG signals have been processed and segmented, 27 features were considered and then combined into five feature sets. All the feature sets were used to train and test three different type of classification: K-Nearest Neighbour (KNN), Support Vector Machine (SVM), and Linear Discriminant Analysis (LDA). Six metrics were used to evaluate the classification performances across all classifiers.

Results and discussion. From this research resulted that the analysis of myoelectric signal is a reliable method to perform handwriting recognition. It resulted that the best classification algorithm for this purpose was the KNN (average accuracy 85%), followed by the SVM (average accuracy 64%) and the LDA, that instead resulted insufficient (37% of average accuracy). Moreover, the best feature set resulted to be that which includes features in time domain, plus the autoregressive coefficients (TDAR feature set). To have the greatest information content for this handwriting pattern recognition problem, it resulted to be essential to combine the myoelectric information coming from wrist and forearm contemporaneously (the 6-channels setup), even if the results coming from the forearm reduced setup are encouraging, with an accuracy of 84% in the case of the KNN, with the TDAR feature set.

1 Introduction

Writing is one of the most diffused actions in daily living. Learned during childhood and regularly practiced, the handwriting becomes a very easy and a natural movement almost for everyone. With passing of years a lot of experience is gained and the writing process also becomes faster and the action more fluid. Writing by hand is a key talent when considering the socio-cultural environment. Being capable to write numbers, letters and sentences by hand is a fundamental skill because it provides the ability to annotate materials and concepts, making it a particularly distributed tool for communication.

Nowadays, with the widespread use of computers and other electronic devices, writing activities require less time. This is because the computer interface is organized in an effective way to make the work, and therefore the writing task, easier and faster. However, handwriting continues to be the most widely utilized and the first writing tool taught from an early age [1]. The act of writing with a pen, appears to be extremely simple and immediate for almost everyone, but upon closer examination of its characteristics, it becomes clear that several regions of the arm are utilized, making it a complex activity requiring the synchronization of numerous muscles and tendons. In order to adapt the movement and ultimately map a graphical sign into a 2D orthographic representation that follows an intelligible writing pattern, the central nervous system must integrate visuo-spatial information and regulate all fine muscle contractions [2]. As a result, there are two main factors that contribute to the inner complexity of handwriting: the involvement of a network of brain structures whose interconnections are writing specific, and the actuator muscles that execute the graphical sign in accordance with the motor commands.

In a right-handed writer, strongly left-lateralized activations are linked to the left hemisphere sensorimotor areas controlling the right hand [3]. The amount of brain area activation is correlated with the complexity of the handwriting task. The coordination of muscles for writing and completing other traditional writing-related activities, such as reading, constructing sentences, and interpreting the meaning of phrases, typically requires a complex synergic activation of several brain zones. It has been shown that handwriting task exhibits high variability between subjects [4]–[6]. The wide range in handwriting styles among people is largely influenced by the writing technique learned as a child, as well as by personal taste, copying peer style variations during adolescence, and later in life by the quantity of writing experience. Because all of this, it is challenging to identify exactly which part of the brain is in charge of pure writing. Most often, the left superior frontal sulcus/middle frontal gyrus area, the left intraparietal sulcus/superior parietal area, and the right cerebellum are thought to be the brain regions that are primarily involved in writing, while others are thought to be involved in non-

specific motor (primary motor and sensorimotor cortex, supplementary motor area, thalamus, and putamen) or linguistic processes (ventral premotor cortex, posterior/inferior temporal cortex) [2]. As said before, the major activation of the brain, and so the major electrical activity of brain, occurs in left hemisphere that is responsible for the control of the right part of the body, so also of then right arm muscles.

Focusing on handwriting and on the circumstances in which someone writes a sentence, it is immediately clear how each writer's writing differs from the other ones. Variability of handwritten track can be observed in the size or in the shape of written symbols, thus same letters may present different height or width. Indeed, the degree of variation depends on the style and speed of writing, with fast writing usually showing less legibility and greater variation [7]. Even if the biggest variety is typically seen between distinct participants, the handwritten track might greatly vary even within a single individual [6]. Considering that the personal writing style can be strongly affected by external environment conditions, like the light conditions or the comfort of the location, but it can be also influenced by internal conditions, like tiredness, hurry, or other psychological conditions, from time to time, the manner of writing can vary greatly. The variability of handwriting includes both the shape of the tracks, but also the method in which each person's actuator muscles execute the writing operation.

Focusing now on the electromyographic (EMG) signals, they are biological signals that are related to muscles contraction which can be recorded and analysed for different purposes. When performing the task of writing a character, one person experiences simultaneous muscular activations that are radically distinct from those of another writer and this, as has been said before, is due to the great variability that is characteristic of handwriting which is therefore also found in the activation of the muscles. Anyway, it is still possible to record those muscular activations and analyse them in the same manner, even if they are recorded from different subjects. In this project, the objective is to create a trustworthy learning model that can recognise handwritten words from EMG data collected at the wrist and forearm levels. The information obtained from the EMG signals can be used for a variety of applications, including real-time handwriting correction, neuromuscular control degeneration therapy and potential recovery.

1.1 Handwriting recognition and applications

Through the method of handwriting recognition, a machine can automatically recognize handwritten letters, symbols, characters, and numbers of every alphabet. It can be used, for handwriting recognition, both online and offline methods. With an online character recognition system, characters are processed as they are being created, and the computer detects the writing as the user types in real time. Online handwriting recognition is becoming more viable for application, especially in pen-input devices like tablets or keypads because to improvements in this technology and recent CPU speed [8]. Online handwriting recognition has a wide range of uses, including reading postal addresses, bank check amounts, and forms. Additionally, online character recognition is crucial for digital libraries because it enables the entry of picture text data into computers using methods for digitization, image restoration, and recognition [9]. In contrast, offline handwriting recognition occurs after the writing is finished. Even though the handwritten signal is analysed after the writer has finished his assignment, it finds a lot of applications in circumstances when a simultaneous response is not required. Offline recognition has the benefit of being possible at any moment after a document has been written. Because only spatial information is accessible for offline systems, whereas both spatial and temporal information is available for online systems, offline handwriting recognition systems are less accurate than online systems [9]. There are primarily three approaches to handwriting recognition: handwriting recognition based on picture analysis of handwritten traces, kinematic analysis, and myoelectric analysis. The distinction between them is that different types of input data are utilized by each method. The first one makes use of 2D character images [10], which are typically acquired by touch screen tablets, the second one utilizes kinematic data, such as acceleration and velocity of hand, wrist, and forearm segments, and the third one uses the data found in EMG signals to identify handwritten characters. While the first and second approaches have gotten a lot of attention in literature, the last approach is novel. EMG signals are frequently employed and used as a control signal in a variety of man-machine interfaces. They are also used in numerous clinical and industrial applications, such as the diagnosis of neuromuscular diseases and the control of assistive devices like orthotics and prosthetics. Analysing the information concealed within myoelectric data is necessary for handwriting recognition using EMG signals. The input for this method is EMG signals, and typically, features are extracted from signal windows after raw signals have been processed. These features are then utilized to train and verify a suitable classifier with the goal of performing pattern recognition [11].

Furthermore, handwriting has come to be regarded as a powerful tool in the rehabilitation of individuals with a variety of diseases. First, in children affected by dysgraphia, which is a learning

disability concerning the mechanical handwriting skill, unrelate to reading or spelling abilities, the rehabilitation it is focused on some handwriting exercises in order to overcome those learning disabilities [12]. Another rehabilitation field in which handwriting is very diffused, it's in patients affected by Parkinson's disease (PD). The PD is a neurodegenerative disorder characterized by the loss of dopaminergic neurons in the basal ganglia leading to a number of motor symptoms [13]. Aside from the primary motor symptoms, handwriting difficulties occur frequently and are generally known as micrographia, i.e., a reduction in writing amplitude [14]. These difficulties commonly result in reduced legibility. Even if it is not the only deficit that this pathology entails, micrographia is one of the important features of handwriting impairment in PD. To assess the utility of handwriting rehabilitation in PD patients who experienced difficulties with handwriting and signing, there are some studies related to an experimental training to help and improve the writing size in those patients [15], [16]. Another important application of handwriting rehabilitation is related to patients after a severe traumatic brain injury, or after the coma. In both cases, the studies focused on the handwriting rehabilitation, show improvements in the condition of the patient, and it seems to progressively help to recover the normal functionalities of the hands [17], [18], [19]. Once it is ascertained the fact that handwriting is an important capacity in various aspects, whether it is used for rehabilitation or for the study of myoelectric signals, to obtain important information for the realization of prostheses that can be used in real time, or for assisted people, it is possible to focus on the studies of the last few years that dealt with the analysis of EMG signals while writing.

1.2 Myoelectric analysis of the upper limb gesture

In literature there are several studies related to the analysis of the hand gesture using myoelectric signals. The study of EMG signals from the hand and forearm during hand gestures has drawn a lot of attention during the past years, and myoelectric analysis of the upper limb gestures has been extensively investigated and requires attention because it can be considered the starting point of the handwriting myoelectric analysis, which is still a novel component that needs additional research and analysis.

Myoelectric control is an advanced technique concerned with the detection, processing, classification, and application of myoelectric signals to control human-assisting robots or rehabilitation devices, and in general to develop human-machine interfaces [20]. The study of Oskoei et al. (2007) reviewed some research and development in pattern recognition and non-pattern recognition-based myoelectric control. As many disabled people have difficulty to access current assistive robotic systems and

rehabilitation devices, which have a traditional user interface, such as joysticks and keyboards, more advanced hands-free human–machine interfaces are necessary. Using surface electrodes, it is possible to decode a user's intention as a muscular contraction from myoelectric signals. It is evident that individuals with disabilities or amputations can produce myoelectric signal patterns that are repeatable but gradually change with varied degrees of static muscle contraction or dynamic limb motion [20]. In the same way, in the study of Micera et al. (2010), attention was devoted to the possibility of using electromyographic signals, recorded either with surface (sEMG) or intramuscular (iEMG) electrodes, on right limb arm amputee patients [21]. In both the previously cited studies, there was a pattern recognition based myoelectric control through algorithms that can automatically recognize patterns and regularities in data. There are indicated all the steps performed regarding the signals acquired, from the data segmentation, the feature selection, the classification until the pattern recognition and applications. All these steps are further investigated and explained in the successive chapters of this manuscript since this is the procedure that it is then utilized in most of the successive studies in this field. In fact, some years later, the same procedure was adopted in the study of Al-Timemy (2013) where, whereas the precedent research was mainly devoted to identifying hand movements as these actions generate strong EMG signals recorded from the forearm [22], in this paper there was the use of multichannel sEMG to classify individual and combined finger movements for dexterous prosthetic control [23]. In the same year, it was proposed the evaluation of the EMG features typically used in the pattern recognition procedure [24], making a distinction between the single feature and multiple feature sets.

For what concern upper limb amputation, this is a condition that severely limits the tasks that amputees may accomplish daily. In this case, the myoelectric prosthesis aims to restore the function of such amputated limbs by using signals from the remaining muscles in the limb. Unfortunately, the collection and use of such myosignals are laborious and difficult. Additionally, it typically takes a lot of processing resources to convert it into a user control signal once it has been obtained.[25] There are numerous issues that make difficult for EMG signals to be converted into a workable prosthetic, particularly those connected to each amputee's differing mobility, muscle contraction forces, limb positioning variations, and electrode placements. The elements, user movement and muscular contraction, affecting the conventional EMG-pattern identification methods could be greatly reduced by modified machine learning schemes for pattern recognition [25]. During the same years, the analysis of EMG signals of upper limb amputee patients was performed in other studies. In the study of Li et al. [26], EMG signals coming from patients with a trans humeral amputation without any form of neurological disease where considered, in the same way in the study of Bai et al. [27], the analysis of user’s intention through non-invasive surface EMG acquisition from the biceps was

recorded. Machine learning algorithms were employed for the pattern recognition approach in both of these investigations, confirming that this method has become more effective for this type of study. Another limitation that has an impact on many people's life is the loss of upper limb movement. Numerous solutions have been developed in response to this issue, ranging from innovative physical rehabilitation techniques to sophisticated biomechanical prosthesis. For this reason, the same approach has been adopted for the study of hand gesture of healthy subjects referring to the evaluation of EMG signals generated by the muscles in the arm, forearm, and hand [22], [28], [29] in order to obtain a solution suitable for real time applications in the cases of amputee patients or for the rehabilitation. In this vein, a very recent study from Covello et al. [30] is based on the use of learning machines that can combine good accuracy with the low memory usage and processing typical of these machine learning models, to promote greater autonomy to users related to one of the main limitations of these applications and recognition of signal patterns for movement classification. To capture the different information from the EMG, it is usually necessary to extract characteristics in the time and frequency domain [20]. However, due to the stochastic nature of the EMG, a small window contains little or no useful information about muscle activity [31]. This means that a sliding window around 150 ms to 250 ms, according to Smith et al. [28], is indicated for a good representation of the signal. In the work from Covello et al. it is proposed a simple method for EMG classification where there is the investigation of some classifier models, such as the multilayer perceptron and linear discriminant analysis. The study it is based on the use of two datasets, the first one including healthy subjects' data and the second one with myoelectric signals from patients with amputation. The results were at the end evaluated as a function of accuracy.

As all this emerges from the studies concerning the EMG signals of the arm, it is possible to shift the attention more specifically to studies that analyse the myoelectric signals in relation to handwriting.

1.3 State of the art in the handwriting recognition by myoelectric analysis

The study of Okorokova et al. (2015) [32] is one of the first studies in literature that concerns a dataset obtained from tasks related to the handwriting of symbols. In this case the writing tasks consisted in 10 different classes, with numbers from 0 to 9, and it is applied the Kalman filter, that is a concept much applied in time series analysis used for topics such as signal processing, for the reconstruction of handwritten pen traces based on EMG signals. Similarly, in a previous study of Linderman et al. [33], the same writing tasks were analysed using EMG signals, and it was demonstrated the feasibility of recreating handwriting solely from EMG signals and this findings could be utilized in computer

peripherals and myoelectric prosthetic devices. Additionally, this strategy might offer a quick and accurate way to identify several neurogenerative diseases before symptoms onset. In fact, in the study of Cascarano et al. [8] it is proposed an innovative set of features extracted by geometrical, dynamical and muscle activation signals acquired during handwriting tasks, focusing of healthy and PD patients. Each involved subject was asked to write three different patterns on a graphic tablet while wearing a commercial armband used to collect the muscle activation signals of the main forearm muscles. With the extraction of the features from the EMG signals and through the analysis with a neural network, it was possible to discriminate healthy patients from PD patients, furthermore the level of the disease too.

In all those studies it was investigated the relationship between handwriting and neuromuscular reactivity measured by electromyography. Further, another important aspect of handwriting was considered. The study of De Almeida et al. [34], was focused on the monitoring of EMG signals of trapezius, biceps brachii, extensor carpi radialis brevis and flexor digitorum superficialis during handwriting tasks, considering that there are different forms to hold the writing objects. The basic idea was to determine the muscles that require the higher energy of activation during handwriting, which resulted to be the proximal muscles. With the crescent substitution of manuscript writing for its digital forms, as computer keyboards and tablets in every life situation, the instruction and monitoring of handwriting development can be overlooked at younger ages. This could result in problems observed in situations that demand intense handwriting production, such as the inability to proper perform university written exams due to significant pain. In 2016, Yang and Chen [35] proposed a way to analyse the EMG signals, coming from 11 different handwritten shapes. This study is then focused on the use of neural network for the classification of the data. The same line was used in successive studies [36], that focused on the comparison between the performance of machine learning and neural network techniques for the classification. In 2020, Beltran-Hernandez et al. [37] analysed the EMG signals while writing with the index finger the 26 letters, lower case, and the 10 decimal numbers. They put forth an innovative method that makes use of deep learning (DL) architectures for feature extraction and sequence recognition. Although the use of such structures produced positive results, with a 94.8% overall classification accuracy, the DL approach was computationally more expensive than machine learning, making it potentially more challenging to use in an online setting. Because of this, selecting an appropriate classifier is a crucial decision that has been discussed in literature. When there is a significant amount of data to process, neural networks (NN) and convolutional NN can be a solution for feature extraction and signal processing. Also, Long Short-Term Memory (LSTM) networks can be employed to recognize sEMG signals, given that LSTMs have been effectively applied to gesture recognition [38]. However, it has been shown that

machine learning techniques are a reasonable alternative in terms of computational load and recognition accuracy [33].

1.4 Aim of the work

The goal of this study is to develop a reliable model that can identify handwritten characters from EMG data acquired at the level of the wrist and of the forearm.

Developing a classification model that allows to distinguish between 30 different handwritten words in cursive. To achieve that, there are some aspects that are investigated in this thesis. To start, the selection of an appropriate electrode setup is crucial when dealing with an EMG pattern recognition challenge and determining the appropriate configuration for the positioning of electrodes over the arm is an essential step for improving the system's multi-class predictive performance when handwritten characters need to be identified.

Furthermore, considering that the way to access myoelectric informational content is through the extraction of EMG signal features, a careful selection and choice of them is necessary to solve pattern recognition problems successfully. For this reason, in this study time domain, frequency domain, and time frequency domain features were evaluated. After a global evaluation of the totality of the features chosen, it was performed the analysis of the most used feature sets in literature, to find which have the best information content.

All those steps are widely explored and explained in the next sections of this manuscript, starting from the setup of the acquisition of the data, the writing task, the signal processing phase, the extraction and aggregation of features and the classification phase. All the results are then reported, and further discussed.

2 Materials and methods

In this section are described in detail all the experimental steps of the present study, from the setup and the writing task, until the signal processing phase, with a focus on the feature extracted and the classification techniques adopted.

2.1 Electromyographic signals

Because the analysis of EMG signals it's a key element in this study, it's of relevance introducing what these kinds of signals are, where they are from and how it is convenient to analyse them. The myoelectric signal is the electrical manifestation of the neuromuscular activation associated with any kind contracting muscle [39]. Even though the analysis in this manuscript relies on EMG signals from the wrist and forearm, the way in which those signals are produced and recorded is independent of the muscle, thus a general description may be given.

A muscle is a type of contractile tissue that is used by animals to generate motion. Human muscular systems are categorised based on their outward appearance and cell placement. The three muscle kinds are smooth, cardiac, and striated or skeletal. For the purpose of this work, it is good to focus just on the skeletal muscles, since they are responsible for the whole-body voluntary movements. A skeletal muscle is made up of a collection of rather long, cylindrical cells with spindle-shaped ends, called muscle fibres. If it is cut transversely, it can be seen that these fibres are not isolated but grouped in bundles and wrapped in connective tissue. The motor unit (MU), which describes the neurological regulation of the muscular contraction, is the smallest functional unit and is composed of the motor neuron, its dendrites and axons and the muscle fibres it innervates. The motor units connected to that muscle are triggered when a contraction of that muscle fibre is necessary. Usually, several motor units collaborate to generate the contraction of a single muscle. When a motor unit is activated by the central nervous system (CNS).

Due to the large number of muscle fibres that make up a motor unit, depending on the probe's spatial distance and precision, the electrode pair can measure the magnitude of all innervated fibres inside this motor unit. By adding the action potentials of the fibres it's possible to obtain the motor unit action potential (MUAP), characterised by a triphasic pattern. Depending on the geometrical fibre orientation in relation to the electrode site, MUAPs vary in shape and size. So, the final EMG signal is created by superimposing all MUAPs (Figure 1).

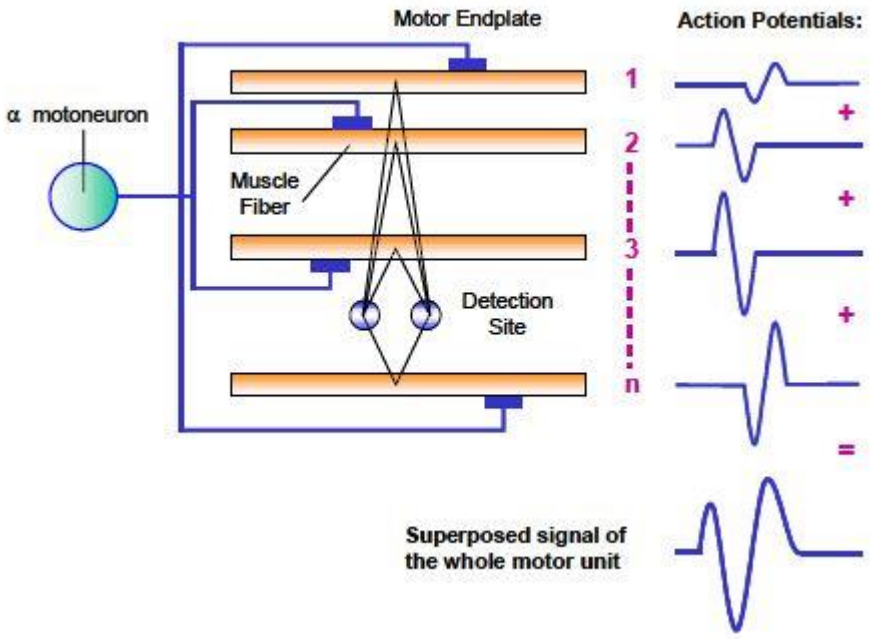

Figure 1: The same detection site can detect n action potentials from different muscle fibres. The amplitude of the action potential decreases with increasing distance between the detecting point and muscle fibre. It is shown the summation of all the action potentials to obtain the final EMG signal of that muscle [40].

The signal obtained from the electrodes it's the raw EMG recording (Figure 2). There are typically four phases in the signal processing procedure, however none are required or strictly necessary [41]. The following conventional processes that an EMG signal can go through, or not, depends on the study's objectives. The step that it's always considered at the beginning when dealing with signals, it's the filtering. With today's technology for acquisition, which already performs a band pass filtering at the level of the amplifier, additional filtering is typically not required for dynamic EMG research. The EMG provides significant information in the band between 10 and 500 Hz. There are scientific recommendations for research studies, i.e., European Recommendations for Surface Electromyography SENIAM, that don't suggest any narrower band setting and in particular, the application of notch filters, to cancel out 50 or 60 Hz noise, is not always recommended because it can compromise too much EMG signal power information.

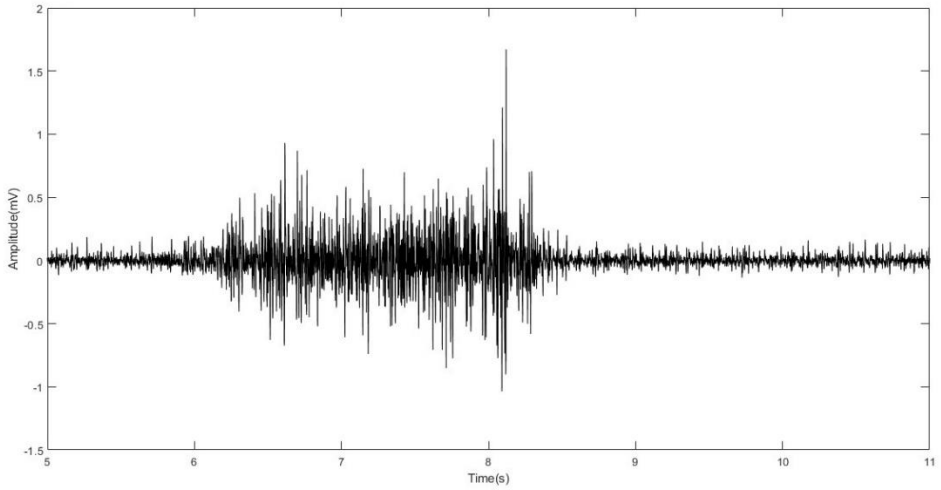

Figure 2: Example of a raw EMG signal.

2.2 Actuators muscles of handwriting

Writing by hand, through the use of a pen on a sheet of paper requires the activation of three groups of muscles: muscles in the forearm, muscles of the hand and the muscles of the upper part of the arm, near the shoulder. However, because to their distinct complexity, it is challenging to analyse the hand movements based on all these muscles. Due to the strong connections present among the muscles in the hand and in the wrist, it is particularly difficult to voluntarily exclude a muscle from the synergy to which it belongs [42]. Thus, for simplification purposes, the hand motion during writing is typically constructed at the wrist and forearm in literature[43], [44]. In Figure 3 are reported anatomical references for the forearm and hand muscles.

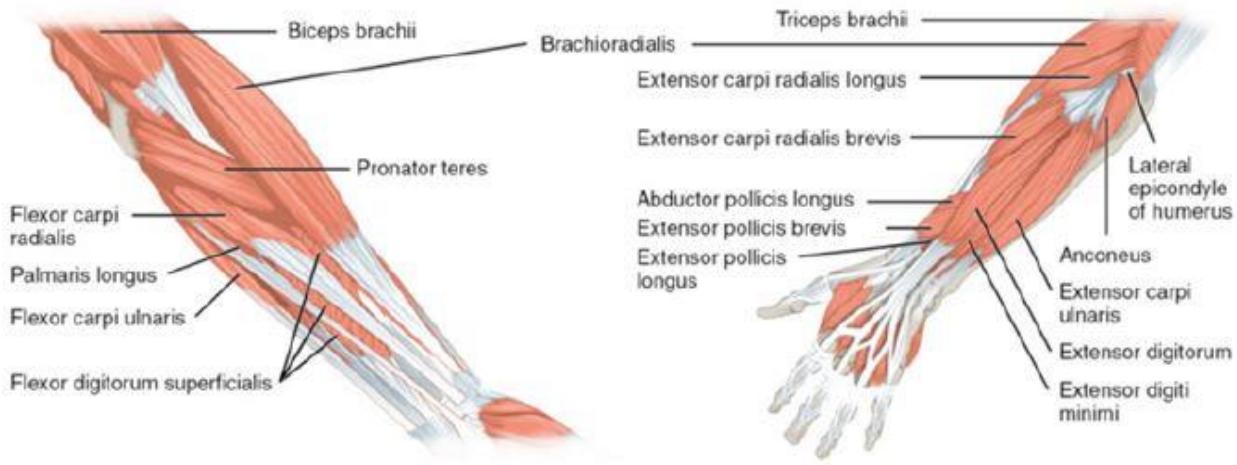

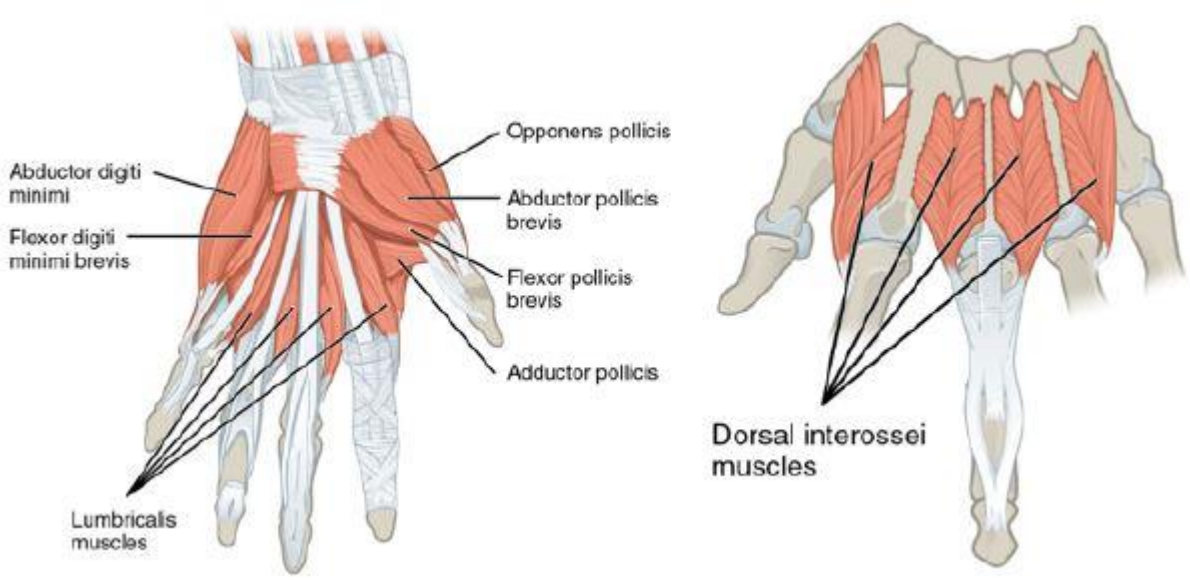

Figure 3: Top panels: muscle of the forearm; on the left palmar view of left forearm superficial muscles. On the right dorsal view of left forearm superficial muscles. Bottom panels: dorsal view of right-hand superficial muscles and of left hand interossei muscles [45].

The forearm muscles can be divided into two macro groups, anterior and posterior muscles:

- The muscles in the anterior compartment of the forearm are organised into three layers (Figure 3, top panels):

  the superficial, composed by flexor carpi ulnaris, palmaris longus, flexor carpi radialis, pronator teres. The intermediate, with the flexor digitorum superficialis. And the deep layer, where there are the flexor pollicis longus, the flexor digitorum profundus and the pronator quadratus [46].

  This muscles group is associated with pronation of the forearm, flexion of the wrist and flexion of the fingers. They are mostly innervated by the median nerve, and they receive arterial supply from the ulnar artery and radial artery [47].
- The muscles in the posterior part of the forearm are commonly known as the extensor muscles. The general function of these muscles is to produce extension at the wrist and fingers. They are all innervated by the radial nerve [47]. Anatomically, the muscles in this compartment can be divided into two layers. The superficial layer where there are the brachioradialis, Extensor Carpi Radialis Longus and Brevis, Extensor Digitorum Communis, Extensor Digiti Minimi, Extensor Carpi Ulnaris, and the Anconeus. And the deep layer which is composed by the

Supinator, Abductor Pollicis Longus, Extensor Pollicis Longus and the Extensor Indicis Proprius [46].

The muscles of the hand (Figure 3, bottom panels) are the opponens pollicis, first dorsal interosseus, medial slip/lateral slip and abductor pollicis brevis [46]. Focusing now again of the handwriting, it has been studied that the radial abduction and ulnar abduction of the wrist joint are commonly used in giving letters width and that the flexion and extension of thumb, index, and second fingers is usually used to give letters their height [38].

2.3 Hardware and setup

After carefully examining the studies in the literature and considering the anatomy of the arm, the first step performed in the present study, it's the definition of the electrodes location. Each subject, before starting the writing task, is correctly prepared and the wrist and forearm are cleaned and dried properly to avoid problems in both positioning and acquisition of the electrodes, then they are armed with EMG electrodes. The electrodes used are BTS Bioengineering FREEEMG (Figure 4), those are surface electrodes, particularly adhesive gel electrodes, to make the positioning easier also in case of errors. Through the use of Wi-Fi technology, connection cables are avoided, allowing for more comfortable handwriting. Their thin and compact size ensures that they are placed precisely over targeted muscles. To be able to prevent any unwanted movement during a dynamic activity that would contribute random noise to the signal, it is crucial to make sure that each electrode is firmly attached to the skin during the placement phase. These electrodes allow for the acquisition of EMG data at a sampling rate of 1000 Hz. In order to prevent cross-talk occurrences, electrodes must also be placed as close as feasible to the muscle's centre while maintaining an inter-distance from one another.
For what concerns the positioning probes methodology, it has been used, for all the subject, one specific designed for the writing task. The setup used was inspired by the studies present in literature previously introduced, particularly the one Botros et al. [43] suggested for a study on hand gesture recognition, to provide the subject with the greatest level of comfort while they are performing the task.
In the current study, it's performed a 6 channel EMG analysis. To cover all the area of interest, the electrodes have been divided between forearm and wrist. In particular, four electrodes are placed at the level of the forearm, all around its circumference, and the remaining two electrodes are located at the level of the wrist in a way to interfere as little as possible with the natural hand's position during writing (Figure 5, a)). The same convention has been respected for all the subjects, making attention

to find every time the same muscles through palpation. In figure 5 b) it's shown the arm of one subject after the placement of the electrodes, in a case of a man. In figure 6 it's shown how, to avoid movement artefacts during the performance of the task, the EMG electrodes are further fixed through the use of medical adhesive tape and tourniquets, in order to lock the electrodes in their correct position without giving the subject any discomfort, in a case of a woman.

Specifically, the electrodes 1 and 4 were placed respectively on the extensor digitorum and on the flexor carpi ulnaris. The electrodes 2 and 3 were located on the anterior part, respectively on the flexor carpi radialis and on the brachioradialis. Those electrodes were located near the elbow, trying to maintain the maximum distance between each other, to avoid crosstalk phenomenon, and at the centre of the muscle of interest. The wrist electrode 5 was placed on the anterior side, over the distal ending of flexor carpi radialis in correspondence of the deep flexor pollicis longus and the wrist electrode 6 was placed in the posterior side, on the extensor digiti minimi. In figure 7 are shown the anatomical references for those muscles. Such electrodes configuration wants to guarantee the widest spatial coverage of the arm, facilitates the recording of EMG signals from bellies of deep layer muscles, involved in the control of fine finger motion, coming to the surface at the wrist level [22], [44].

Figure 4: On the right, Charging box BTS electrodes. When batteries are completely charged, electrodes guarantee up to 6 hours of nonstop acquisition. On the left, a focus on one BTS surface electrode. Its small dimension and the absence of wires makes it suitable for handwriting task.

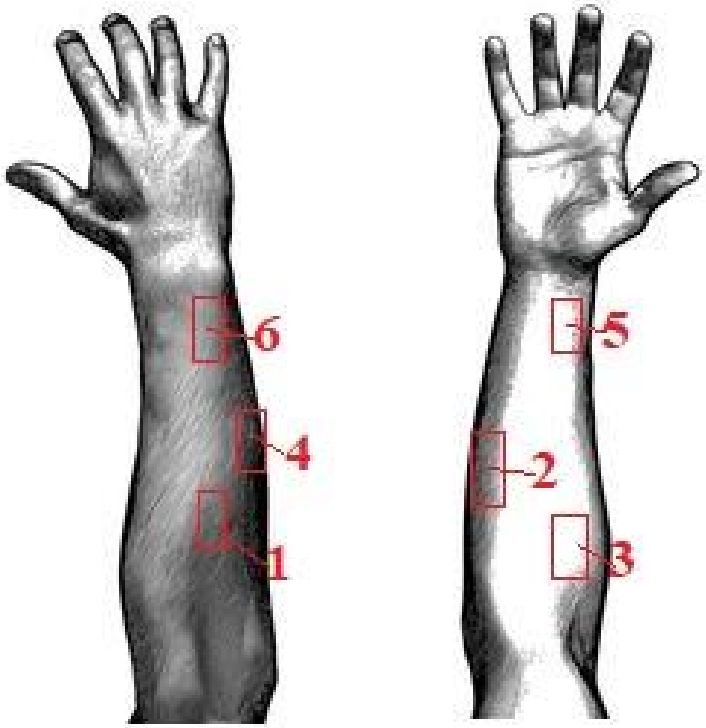

a)

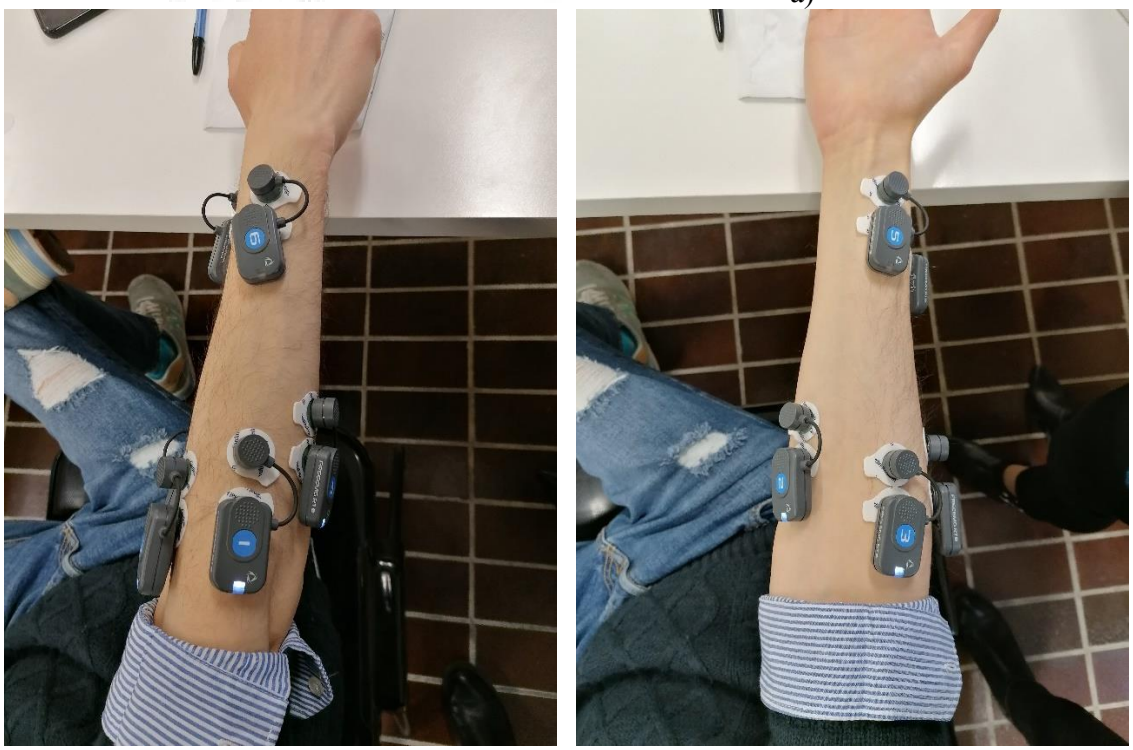

b)

Figure 5: a) Setup of the electrodes adopted for handwriting recognition task. On the left, posterior view of the right arm; on the right, anterior view. b) Right arm of one subject after the placement of the electrodes.

Figure 6: Setup of the electrodes, further fixed using medical adhesive tape and tourniquets, in order to lock the electrodes in their correct position during motion.

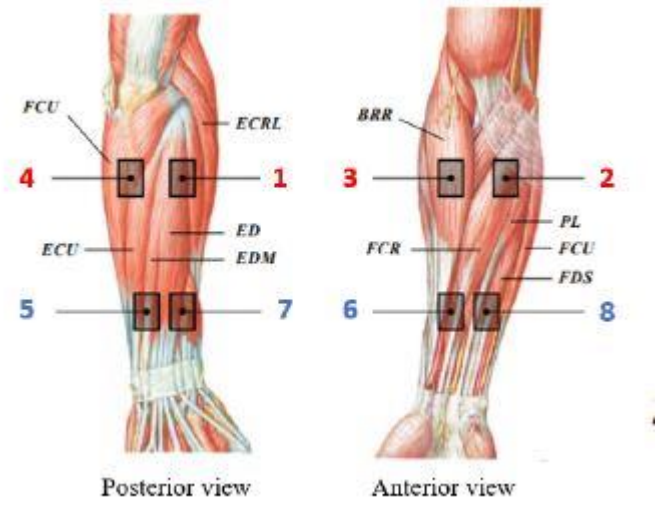

Figure 7: Anatomical references for the muscle's activity recorded, anterior and posterior view. Forearm electrodes 1,2,3,4 and wrist electrodes 5,6 (corresponding respectively in this representation to the 6 and 7). BRR: brachioradialis; ECRL: extensor carpi radialis longus; ECU: extensor carpi ulnaris; ED: extensor digitorum; EDM: extensor digiti minimi; FCR: flexor carpi radialis; FCU: flexor carpi ulnaris; FDS: flexor digitorum superficialis; PL: palmaris longus. Figure adopted by [43].

2.4 Definition of handwriting task

This experiment was performed by 6 healthy subjects, 3 men and 3 women, aging between 25 and 40 years old. One of them was left-handed, all the others are right-handed. The subjects were instructed to make themselves comfortable before beginning to write, and to try to write a few words, if necessary, to become trained. All participants were then asked to write through a pen on a sheet of paper, 30 words, with their natural way of writing in cursive. Each of the words were then repeated 10 times, sitting in a comfortable position, and leaning the arm against desk to not feel fatigue during the task, as shown in figure 8. Approximately, were necessary 2 minutes to write down all the 10 repetitions of a single word, for a total duration of the task of around one hour. After the first 10 words have been written, a 5-minute break is taken to rest the subject and in the same way if the person needed more breaks.

The writing and rest phases during the task, were marked by a timer giving 5 seconds for writing the word and 5 seconds of rest between each repetition. For each subject, the words that must be written were always the same, and they were divided in 10 nouns, 10 adjectives and 10 verbs, reported in figure 9, considering the most common English terms [48], ranging from 2 to 10 letters [49].

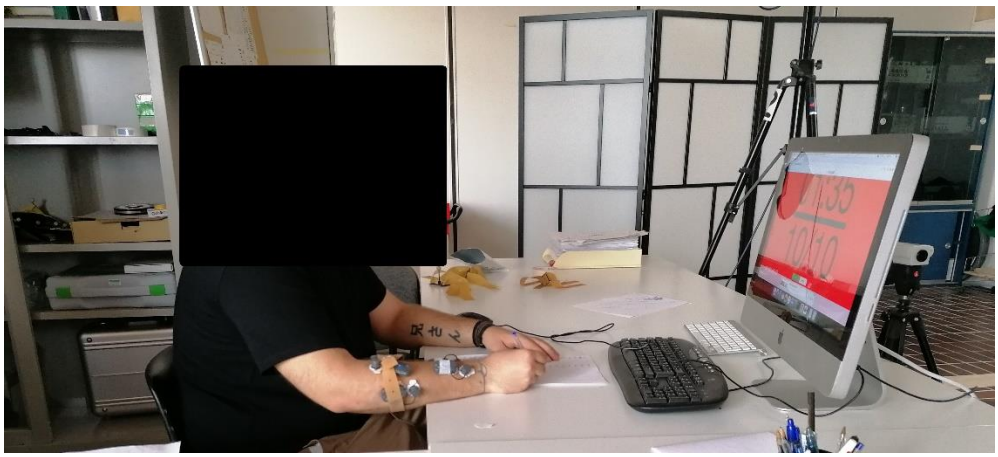

Figure 8: Two participants while performing the task. After finding the comfort position, they follow the timer for the writing.

	Nouns	Adjectives	Verbs
1	time	good	be
2	person	new	have
3	year	first	do
4	way	last	say
5	day	long	get
6	thing	great	make
7	man	little	go
8	world	own	know
9	life	other	take
10	hand	old	see

Figure 9: The 30 most common English terms divided in 10 nouns, 10 adjectives and 10 verbs [55].

2.5 Raw EMG signal

An example of the raw EMG signals obtained from the muscle activation recordings is shown in figure 10. When the muscle is relaxed, it's possible to see a quite flat EMG baseline where the noise components depend on different factors, like the environment noise, the quality of the detection conditions and of the EMG amplifier. It's possible to observe 10 bursts, correspondent to the time required by the subject to write down the single word. The writing phases on average are around 3000 samples long, and the resting phase is given by 5000 samples. From the recording of a single multi-channel, 6 tracks are recorded and can be visualized, as shown in figure 11.

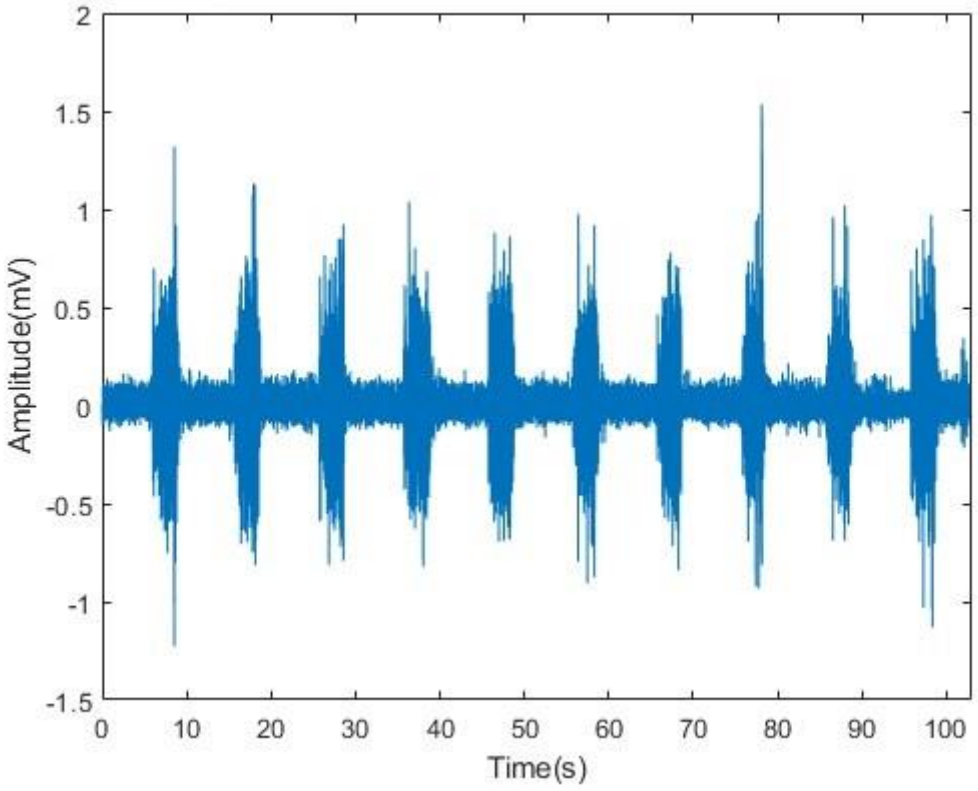

Figure 10: Raw EMG signal from the subject number 4. This recording is related to the writing of the word "little" and on the activation of the flexor carpi radialis.

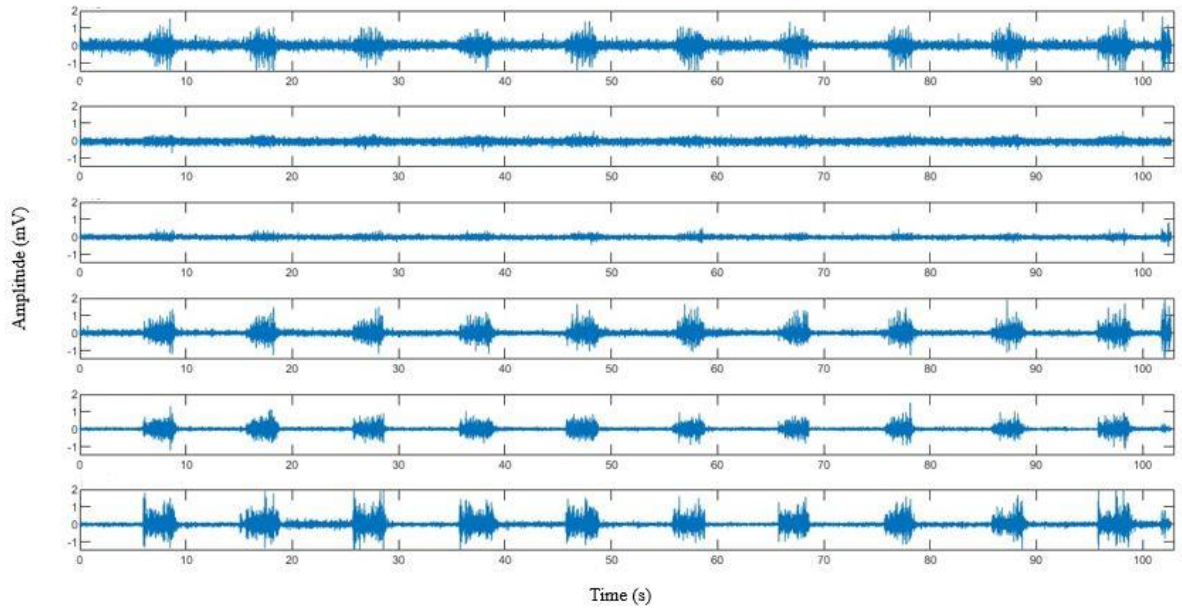

Figure 11: The 6 channels recording of a single writing task. The writing of the word "little" from the subject number 4. One single acquisition includes 6 channels recording, as shown in figure. Each channel, here shown in rows, refers to an electrode sensing electrical activity of a different muscle or a group of muscles. On the x-axis are indicated the number of samples, on the y-axis the amplitude of the signal in mV.

2.6 EMG signal processing

The raw EMG signal was first normalized. Since all data were divided by the maximum amplitude value discovered during the contraction time, signal amplitude was normalized regarding the maximum peak value. The signal obtained was characterized by the same structure of the original signal, but its amplitude was scaled to have a smaller range between 0 and 1. This is the peak dynamic approach and it's widely used, particularly in studies on gait analysis [50], [51]. In fact, this technique makes it easier to compare the electrical patterns of various muscle groups within a subject and reduces subject variability as much as feasible. Since it was needed to compute features that take into consideration values below the baseline, such zero crossing, signals were not rectified. In addition, a second order bandpass Butterworth filter, with a higher cut off frequency of 450 Hz and lower cut off frequency of 30 Hz, was used. After that, to perform the analysis on the muscle activation, it was needed to know the time instants in which the activation started and the instant in which instead it ended, for every repetition of each word. Hence, it was performed a manual detection of the activation samples, an ON-OFF detection for each repetition (figure 12). For each trial, it was chosen the signal with the lowest SNR among the 6 channels recorded. Based on that, then there was the selection of

10 successive ON values, where the signal presented higher spikes as shown in figure 16, and then it was added to these values 3000 samples to obtain all the OFF values. For each word, in this way, ten windows were extracted from the original signal, each long 3 s (figure 13). The same ON-OFF values detected from the cleanest channel recorded, were then used for extracting the same windows of signal on the remaining 5 channels (figure 14). At the conclusion of this operation, all of the windows were arranged in a 10×6 array, 10 activations for 6 recording channels.

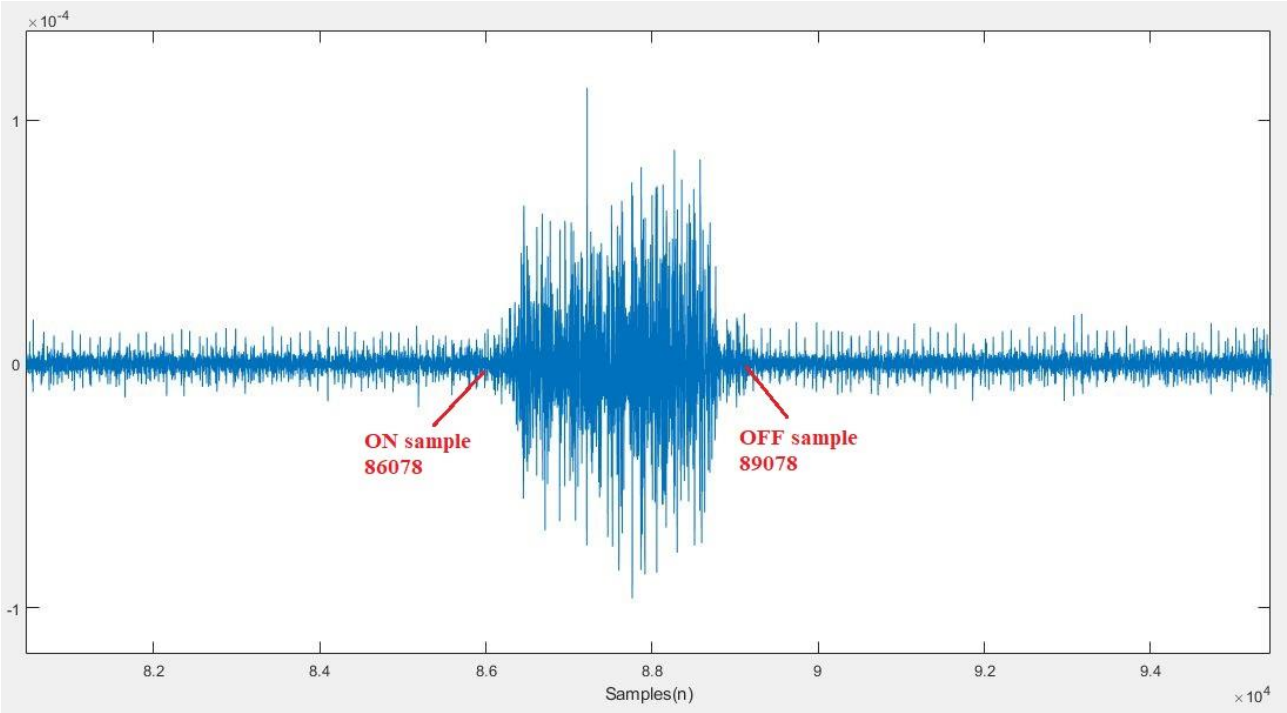

Figure 12: Selection of ON and OFF values (in samples) indicating the beginning and the end of the muscular contraction phase. EMG recording of the channel number 5, related to the writing of the word “day” by the subject number 4.

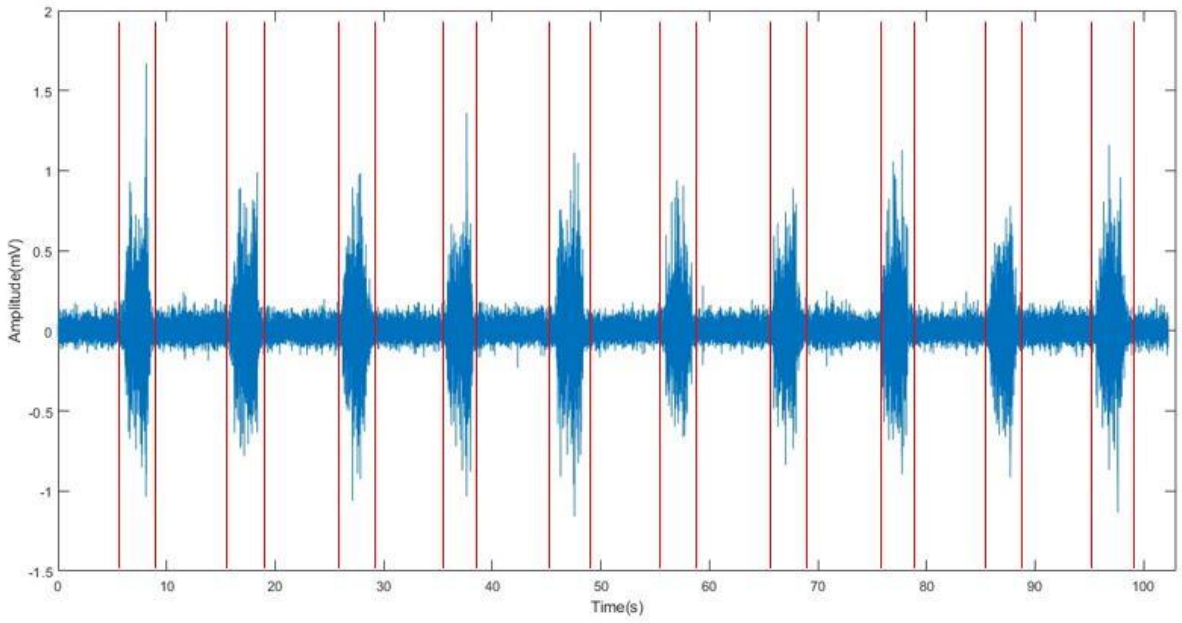

Figure 13: Selection of all writing phases in one single channel. 10 activation windows are extracted. EMG recording of the channel number 5 related to the writing of the word “old” by the subject number 4.

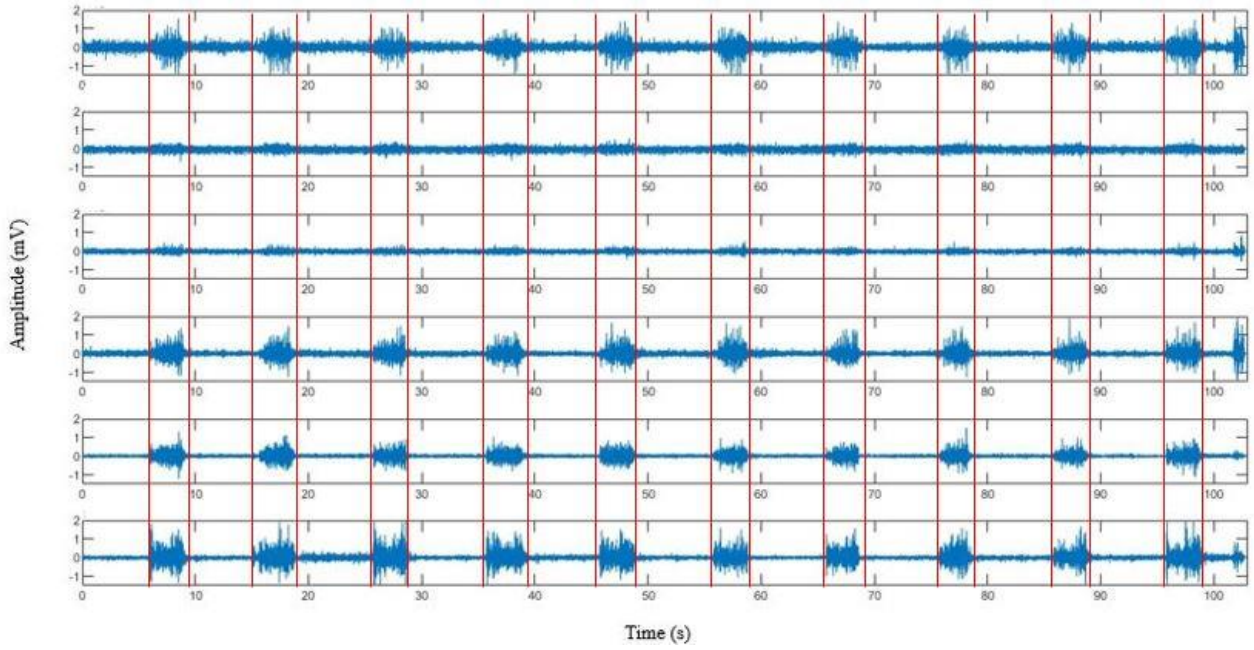

Figure 14: The activation of all 6 EMG channels is detected. Signals related to the writing of the word “little” from the subject number 4.

2.7 Segmentation of signal and feature extraction

The windowing methods are frequently used in myoelectric pattern recognition problem [25]. Windowing basically consists in splitting the entire signal into manageable pieces from which the desired features can be extracted. In the pattern recognition systems, there are primarily two types of windowing methods: adjacent windowing and overlapping windowing.

In adjacent windowing, windows are taken to a certain length and each following window begins at the end of the previous one. These windows are then used for the extraction of the features. However, this windowing method does not provide a dense array of signals, and it's possible that not enough information is being used [52]. In an overlapping window approach (Figure 15), instead, a predetermined window length that typically is stated as a percentage of the global window length, is selected, which slides along the entire signal with an increment size that is smaller than the initial window size[53].

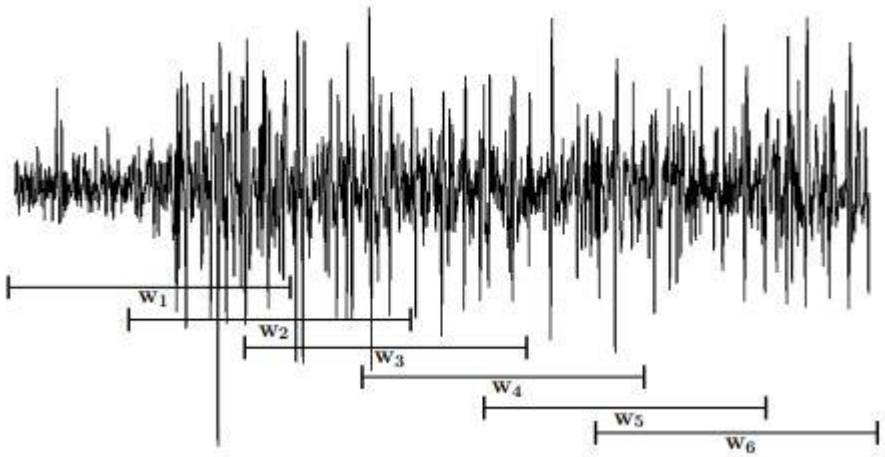

Figure 15: Overlapping window technique for a given EMG signal [52].

Since the size of the window directly affects the total recognition performance, the window length is crucial. The classification accuracy is often higher for larger window sizes [22]. In fact, more data will produce features with reduced variance and, as a result, more accurate classification [22]. The trade-off should be between a real-time latency and classification accuracy because huge window sizes are substantially more expensive in terms of computational burden, extracting features from large windows requires more power and time. Generally, window widths should be assessed considering the particular task under investigation. However, due to real-time constraints, a segment length plus the processing time of generating classified control commands, should typically be equal

to or less than 300 ms in pattern recognition situations [54]. Furthermore, more recent research indicates that the window size should be kept between 100 and 250 ms for best results [28], [55].
In this study, the window size was set at 150 ms, with a 75 ms of overlap, which corresponds to the 50% of the window dimension. Following this, it was possible to proceed with the feature extraction.
The selection of the appropriate features has a significant impact on the pattern recognition issues. This is why one of the most important steps in the design of myoelectric control and pattern recognition is defining the selection and extraction of the effective features. Features is a way of representing raw myoelectric signals for classification, so the success of any pattern recognition problem depends almost entirely on the selection and extraction of features. Time and frequency are the two domains that are considered the most in feature extraction. Further, there is another category, the time-frequency representation category, that combines the time and frequency domains.
In the current study, from each signal segment, 27 features have been retrieved: 16 in the time domain, 10 in the frequency domain, and 1 in the time scale domain, all reported in Table 1.

2.7.1 Time-domain features

The most popular features in myoelectric classification are the time-domain features. They are of fast implementation and easy to compute because they don't need any domain transformation.
In this study, the choice of the feature to be extracted was highly assessed based on the literature and other studies connected to the EMG analysis through feature evaluation for pattern recognition of the upper limbs [8], [35], [36], [56], [57]. All the time-domain features extracted and evaluated in the present work are now listed and briefly described.

- The integrated EMG (IEMG) is the first feature extracted. It's defined as the summation of absolute values of the EMG signal amplitude, and it can be expressed as:

$$IEMG = \sum_{i=1}^{N} |x_i| \tag{1}$$

where x_i represents the EMG signal samples in a segment i and N denotes length of the EMG signal.

- One of the most used in EMG signal analysis, it's the mean Absolute Value (MAV) [56]. It is the average of absolute value of the EMG signal amplitude in a segment:

$$MAV = \frac{1}{N}\sum_{i=1}^{N}|x_i| \tag{2}$$

- The variance of EMG (VAR) [56] is defined as the average of square values of the deviation of that variable. However, the mean value of EMG signal is close to zero and the variance of the EMG signal is typically defined as:

$$VAR = \frac{1}{N-1}\sum_{i=1}^{N}x_i^2 \tag{3}$$

- Another frequently used feature is the root Mean Square (RMS) [11], [56], [58]. It is modelled as amplitude modulated Gaussian random process whose relates to constant force and non-fatiguing contraction. RMS in formulas is:

$$RMS = \sqrt{\frac{1}{N}\sum_{i=1}^{N}x_i^2} \tag{4}$$

- The waveform Length (WL) [30],[56] is defined as the cumulative length of the EMG waveform over the time window and it is computed as:

$$WL = \sum_{i=1}^{N-1}|x_{i+1} - x_i| \tag{5}$$

- The Difference Absolute Mean Value (DAMV) is defined as WL divided by length N minus one. In formulas:

$$DAMV = \frac{1}{N-1}\sum_{i=1}^{N-1}|x_{i+1} - x_i| \tag{6}$$

- The Difference Absolute Standard Deviation Value (DASDV) [56] is similar to RMS feature, it is a standard deviation value of the wavelength that can be defined as:

$$DASDV = \sqrt{\frac{1}{N-1}\sum_{i=1}^{N-1}(x_{i+1} - x_i)^2}$$

(7)

- The Zero Crossing (ZC) [8], [30], [56] describes the number of times that amplitude values of the EMG signal cross zero amplitude level.

$$ZC = \sum_{i=1}^{N} [sgn(x_i \cdot x_{i+1}) \cap |x_i - x_{i+1}| \geq treshold],$$

(8)

$$sgn(x) = \begin{cases} 1, & if \ \ x \geq treshold \\ 0, & otherwise \end{cases}$$

where threshold condition is implemented to avoid low voltage fluctuations or background noises. The threshold value for ZC and the three following features (MYOP WAMP and SSC) was set to 0.001.

- The myopulse percentage rate (MYOP) [56], [59] is an average value of myopulse output which is defined as one when absolute value of the EMG signal exceeds a pre-defined threshold value:

$$MYOP = \frac{1}{N} \sum_{i=1}^{N} |f(x_i)|,$$

(9)

$$f(x) = \begin{cases} 1, & if \ \ x \geq treshold \\ 0, & otherwise \end{cases}$$

- Wilson amplitude (WAMP) [56] , [60], [61] describes number of times resulting from difference between the EMG signal amplitude among two adjoining segments that exceeds a pre-defined threshold. Moreover, it is strictly related to the firing of MUAPs and muscle contraction force. It is defined as:

$$WAMP = \sum_{1}^{N-1} [f(|x_n - x_{n-1}|)];$$

(10)

$$f(x) = \begin{cases} 1, & if \ \ x \geq treshold \\ 0, & otherwise \end{cases}$$

- The Slope Sign Change (SSC) [56], [61] is the number of times that the slope of the EMG signal changes sign. The number of changes between the positive and negative slopes among three sequential segments is performed with a threshold function. It is expressed as:

$$SSC = \sum_{2}^{N-1} \left[f[(x_i - x_{i-1}) \times (x_i - x_{i+1})] \right];$$

(11)

$$f(x) = \begin{cases} 1, & if \ \ x \geq treshold \\ 0, & otherwise \end{cases}$$

- The Fuzzy Entropy (FuzzyEN) [42], it's a measure of the time-series complexity, providing the conditional probability that two vectors recognized as similar for *m* samples remain similar for the next *m + 1* samples as well. It is defined as:

$$FuzzyEN(m, n, r) = ln\phi_m(r, n) - ln\phi_{m+1}(r, n)$$

(12)

where $\phi_m(r, n)$ is a function that considers the degree of similarity between embedding vector z_i and *z-j*.

- Weighted Permutation Entropy (WPermEN) [62] has been recently suggested as a novel measure to characterize the complexity of nonlinear time series and it can be calculated as:

$$WPermEN = -\sum_{i=1}^{d!} p_\omega(\pi_i) \ln(p_\omega(\pi_i))$$

(13)

where the relative frequencies of all the possible permutations π are computed, thereby producing an ordinal pattern probability distribution.

$$P = \{p(\pi_i)\} \qquad i = 1,2, \dots, d!$$

(14)

- The Histogram of EMG (HIST) [56], [60], [61] divides elements in the EMG signal into *N* equally spaced segments and returns number of signal elements for each segment.

- The Auto-Regressive coefficients (AR) model the individual EMG signals as a linear auto-regressive time series and provide information about the muscle's contraction state. In EMG signal classification, coefficients of the AR model a_p, have been used as a feature vector. The

model is a 4th order model, as recommended in literature [56], [60], [61], hence four AR values are calculated for each signal window and used as features. The equation model is:

$$x_i = \sum_{p=1}^{p} a_p x_{i-p} + \omega_i \tag{15}$$

where P is the order of the model and ω_i is a term that considers white noise.

- The Cepstrum Coefficients (CC) [56], [59], [61] were at the end calculated as last time-domain features. A cepstrum of a signal is the result of taking the Fourier transform of the decibel spectrum as if it were a signal. This measure provides information about the rate of change in different frequency spectrum bands of a signal. Cepstrum coefficients are derived from the autoregressive model and calculated as:

$$c_1 = -a_1$$
$$c_i = -a_i - \sum_{n=1}^{i-1} (1 - \frac{n}{i}) a_n c_{i-1} \tag{16}$$

where a_i is the *i*th AR coefficient, c_i is the *i*th Cepstrum coefficient and *i* is the dimensionality of the model. A great advantage of CC is that this feature is computed very fast, since it does not require Fourier transform, hence it is still considered a time-domain feature.

2.7.2 Frequency-domain features

Since the EMG signal's spectrum contains useful information in a time-invariant manner, the pattern recognition issues can benefit from its use. One important and common frequency domain analysis tool, it's the power spectral density (PSD). The PSD of a signal provides an estimation of the power distribution across the whole frequency range. There are two main methods for calculating PSD. The first, and most widely used approach, is the periodogram. It can be calculated by dividing the square of the signal's Fourier transform's absolute value by its length. By averaging the spectra of close windows, under the presumption of stationarity over these windows, the standard deviation of the PSD, estimated at each frequency, is thus equal 100% of the predicted value and may be decreased. The second method for the calculation of the PSD is the model-based or parametric. Under the premise that the signal is a realisation of a stochastic process, it makes use of a mathematical model.

The signal is modelled by treating it as stationary within the current time windows. One of the most popular model for spectral estimation has been the auto-regressive one [63]. As previously done for all the time-domain features, are now listed below all the frequency-domain features evaluated in the present work.

- The Mean Frequency (MNF) [20], [56] is the average frequency which is calculated as the sum of the product of the EMG power spectrum and the frequency, divided by the total sum of the spectrum intensity. It is calculated as:

$$MNF = \frac{\sum_{j=1}^{M} f_j P_j}{\sum_{j=1}^{M} P_j} \tag{17}$$

  where f_j is the frequency of the spectrum at frequency bin j, P_j is the EMG power spectrum at frequency bin j, and M is length of the frequency bin.

- The Median Frequency (MDF) [20], [56], [59] is the frequency at which the spectrum is divided into two regions with equal amplitude. It is defined as:

$$MDF = \frac{1}{2}\sum_{j=1}^{M} P_j \tag{18}$$

- The Peak Frequency (PKF) [56], [59] is the frequency value at which the maximum power occurs. It can be expressed as:

$$PKF = \max(P_j), \qquad where\ j = 1, \dots, M. \tag{19}$$

- Total Power (TTP) [56], [59] is defined as the simple summation of powers of every frequency bin. It is calculated as:

$$TTP = \sum_{j=1} MP_j \tag{20}$$

- The 1st, the 2nd and the 3rd Spectral Moment (SM) [56], [59] are an alternative possibility to extract feature from a PSD estimate. From literature results that the most important spectral

moments are the first three moments [64], hence this feature contain 3 sub-features, that are SM1, SM2 and SM3. It is possible to obtain them as:

$$SM1 = \sum_{j=1}^{M} P_j f_j \tag{21}$$

$$SM2 = \sum_{j=1}^{M} P_j f_j^2 \tag{22}$$

$$SM3 = \sum_{j=1}^{M} P_j f_j^3 \tag{23}$$

- The Frequency Ratio (FR) aims to distinguish between contraction and relaxation of muscle using the ratio between the low frequency components and the high frequency components of the EMG signal [56], [59]. It is calculated as:

$$FR = \frac{\sum_{j=LLC}^{ULC} P_j}{\sum_{j=LHC}^{UHC} P_j} \tag{24}$$

where ULC and LLC are upper and lower cut-off frequency of the low frequency band and UHC and LHC are the upper and lower cut-off frequency of the high frequency band, respectively.

- The Power Spectrum Ratio (PSR) [56], [59] is defined as the ratio between the energy P_0, which is nearby the maximum value of the EMG power spectrum, and the energy P, which is the whole energy of the EMG power spectrum. In formulas:

$$PSR = \frac{P_0}{P} = \frac{\sum_{j=f_0-n}^{f_0+n} P_j}{\sum_{j=-\infty}^{\infty} P_j} \tag{25}$$

- The last frequency-domain extracted is the Variance of Central Frequency (VCF) [56], [59]. It is derived from the spectral moments, and it is calculated as:

$$VCF = \frac{SM1}{SM0} - \left(\frac{SM1}{SM0}\right)^2$$

(26)

2.7.3 Time-frequency features

A major disadvantage of the Fourier Transform is that it captures the global frequency information, meaning frequencies that persist over the entire signal. In other words, the Fourier Transform in spectrum analysis ignores time domain information, making it hard to pinpoint the precise moment that an event occurs. If the signal under analysis is steady, and its characteristics do not change over time, it is considered appropriate, but this kind of signal decomposition may not serve all applications in a correct manner, for example when dealing with EMG signals. Myoelectric signals in fact, exhibit a variety of non-stationary or transient properties and it is impossible to localize the correct instant when a particular event happens through the Fourier Transform.

A first solution to this problem can be obtained applying the short-time Fourier transform (STFT). It maps the input into a two-dimensional function of time and frequency, but only manages to retrieve this information with a degree of precision that is excessively dependent on the window length selected. An alternative and widely used time-frequency approach, it's to apply the Wavelet Transform (WT) to the signal, as it allows for the execution of local analysis. In some cases, wavelet analysis can disclose elements of the data that other methods can't, like allowing following trends or recognizing breakdown spots and discontinuities in higher derivatives.

The WT basically, by scaling and translating a wavelet function, that is a wave-like oscillation localized in time, over the entire signal, as illustrated in figure 16 [65], iteratively converts the signal of interest into multi-resolution subsets of coefficients. The scaling function considered in this work is Coiflet 5 and it's shown in figure 17 [66]. Scale and location are the basic characteristics of wavelets. How a wavelet is "stretched" is determined by its scale and the location identifies the wavelet's position in time. After this first step, a high-pass and a low-pass filters are applied to the original EMG signal to perform, at the first level, both a detailed coefficient subset (cD1) and an approximation coefficient subset (cA1) [67]. Usually, it is requested to reach more than the first level of decomposition alone, and to undertake a multi-level analysis repeated transformations are used until the desired levels of decomposition are reached. If the decomposition level is set to 3, WT will produce the coefficient subsets at the third level approximation (cA3) and the first to third level details (cD1, cD2, and cD3). These four level values are modified into a single feature vector and used as features.

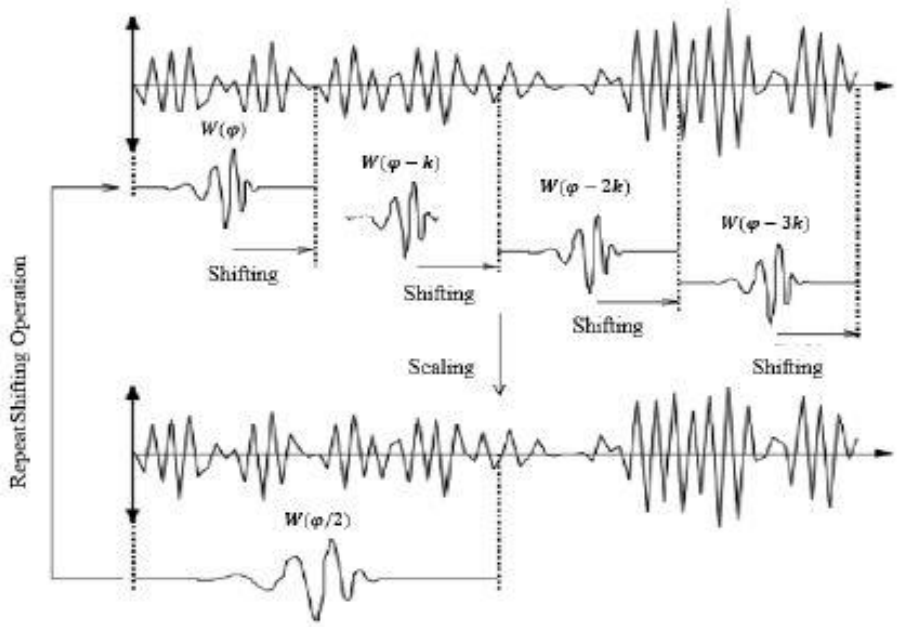

Figure 16: The Coiflet wavelet function is shifted all over the signal length and it's scaled to adapt its shape to the sEMG pattern.

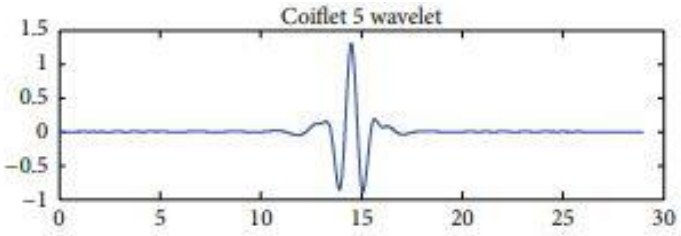

Figure 17: Coiflet 5 function.

Feature extracted	
Time-domain	Integrated EMG (IEMG)
	Mean Absolute Value (MAV)
	Variance of EMG (VAR)
	Root Mean Square (RMS)
	Waveform Length (WL)
	Difference Absolute Mean Value (DAMV)
	Difference Absolute Standard Deviation Value (DASDV)
	Zero Crossing (ZC)
	Myopulse percentage rate (MYOP)
	Wilson amplitude (WAMP)
	Slope Sign Change (SSC)
	Fuzzy Entropy (FuzzyEN)
	Weighted Permutation Entropy (WPermEN)
	Histogram of EMG (HIST)
	Auto-Regressive coefficients (AR)
	Cepstrum Coefficients (CC)
Frequency-domain	Mean Frequency (MNF)
	Median Frequency (MDF)
	Peak Frequency (PKF)
	Total Power (TTP)
	Spectral Moment (SM1, SM2, SM3)
	Frequency Ratio (FR)
	Power Spectrum Ratio (PSR)
	Variance of Central Frequency (VCF)
Time scale	Wavelet Transform coefficients (cA3, cD1, cD2, cD3)

Tabella 1: All the 27 features retrieved from each EMG signal segment are reported with their name and abbreviation: 16 in the time domain, 10 in the frequency domain, and 1 in the time scale domain.

2.8 Feature selection and feature aggregation

All the time-domain, frequency-domain, and time-frequency domain features, they were arranged in a matrix with a number of rows corresponding to the total number of segmented windows and a number of columns corresponding to all the features computed for each channel. When all the features have been arranged in this matrix (with dimensions 14700×264), the following step is the features aggregation. It consists in splitting the features in different sets. In general, a robust EMG feature set it is composed by a combination of features that provide a good separation among data and high classification accuracy. Five feature sets were considered in this work, as reported in Table 2, and were proposed by different studies in literature focused on the classification of myoelectric patterns. The first feature set examined is the one proposed by Hudgins et al. [68] and it's composed by four features, all in the time domain: MAV, WL, SSC, ZC. The second feature set comes from the study of Du et al [69], and it's characterized by 6 features, all in the time domain: IEMG, VAR, WAMP, WL, SSC, ZC. After that, are considered two feature sets proposed by the studies of Phinyomark et al. [14], [59]. The set 1 is composed by five time-domain and two frequency-domain features: MAV, WL, WAMP, ZC, AR, MNF and PSR. The set 2 it's composed by four time-domain features: WPermEn, CC, RMS and WL. After that, the last feature set considered is the Time Domain features combined with Autoregressive model coefficients (TDAR) [70]. It is composed by seven features: MAV, SSC, WL, VAR, WAMP, AR, ZC.

FEATURES SETS	
1) HUDGINS	MAV, WL, SSC, ZC
2) DU	IEMG, VAR, WAMP, WL, SSC, ZC
3) PHINYOMARK SET 1	MAV, WL, WAMP, ZC, AR, MNF, PSR
4) PHINYOMARK SET 2	WPermEn, CC, RMS, WL
5) TDAR	MAV, SSC, WL, VAR, WAMP, AR, ZC

Table 2: The features sets considered are reported, expressing the features that compose them.

Before starting the successive steps, it was performed the splitting of the EMG signals coming from the forearm with respect the EMG signals coming from the wrist's muscles. At this point all the features were organised in two different matrices, still having as number of rows the total number of segmented windows and as number of columns all the features related to each of the channels considered (4 in the case of the forearm and two in the case of the wrist). Once obtained those 3 matrices where all the features are considered (the matrix one, composed by the features obtained by considering all the six EMG signals recorded; the matrix two, composed by the features obtained from the 4 EMG signals of the forearm; the matrix three, characterized by the features extracted from the 2 EMG signals coming from the wrist), the five feature sets are considered for each of the cases, obtaining in this way 5 subcases (each composed by three matrices, one from all the EMG signals, one from the forearm and the last from the wrist, where the five feature sets are considered one by one), to be analysed in the successive step of the classification. Before giving the features extracted to the classification algorithms, all the feature matrices considered were normalized in the range between 0 and 1.

2.9 Machine learning classification algorithms

All the subcases previously described have been used to train and test different classification models. In detail, the 70% of the data were used for the training of the classification models, and the remaining 30% was used for the successive testing step.

Firstly, the classification algorithms chosen were used on the globality of the features and on the feature sets extracted from the signals of each subject, where the data from the forearm and the wrist are analysed like a whole and then separately. As final step, for the inter subject analysis, the data coming from all the six subjects were considered together.

In this work, supervised machine learning approaches have been adopted to perform the pattern recognition and the classification. Three well known classification algorithms have been chosen: Linear Discriminant Analysis (LDA), Support Vector Machine (SVM) and K-Nearest Neighbours (KNN).

2.9.2 Linear Discriminant Analysis

The foundation of the LDA is the idea of looking for a linear combination of variables and predictors, that best distinguishes between two or more classes. This algorithm's primary goals are to maximise inter-class distance and reduce within-class variance. Due to its effective categorization of the EMG signal, robustness in long-term effects, low computational cost, quick training time, and intuitive structure [71], the LDA classifier has been used in this investigation.

LDA makes two simplifications regarding the data: first that the data follow a Gaussian distribution, and then that each variable deviates from the mean value by the same average amount. The LDA model is in this way capable to estimate the mean and the variance from the data, for each class under these assumptions.

The mean value of each input (x), for each class (k), can be calculated in the conventional manner by dividing the sum of values by the total number of values:

$$m_k = \frac{1}{n_k}\sum_{i=1}^{n_k} x_i \tag{27}$$

where m_k is the mean value of x for the class k, n_k is the number of instances with class k [72]. The variance is calculated across all classes as the average squared difference of each value from the mean, as reported here:

$$\sigma^2 = \frac{1}{n-k}\sum_{i=1}^{n_k}(x_i - m_k)^2 \tag{28}$$

where σ^2 is the variance across all inputs x, n is the number of instances, k is the number of classes and m is the mean for input x [72]. To describe it simply, LDA predicts by calculating the likelihood that a new set of inputs belongs to each class. The output class is the one with the highest probability, and a prediction is produced. Using the probability of each class and the probability of the data belonging to each class, the Bayes theorem is used to estimate the probability of the output class k given the input x:

$$P(Y = x|X = x) = \frac{(\pi_k f_k(x))}{\sum(\pi_l f_l(x))} \tag{29}$$

Where π_k refers to the base probability of each class k observed in training data [72]. In Bayes theorem this is called the prior probability and it is defined as:

$$\pi_k = \frac{n_k}{n}$$

(30)

The *f(x)* above is the estimated probability of *x* belonging to the class. A Gaussian distribution function is used for *f(x)*. Discriminant function is finally determined as:

$$D_k(x) = x\left(\frac{m_k}{\sigma^2}\right) - \left(\frac{m_k^2}{2\sigma^2}\right) + \ln(\pi_k)$$

(31)

Where $D_k(x)$ is the discriminate function for class *k* given input *x*, the m_k, σ^2 and π_k are all estimated from data [72].

2.9.3 Support Vector Machine

A SVM is an extremely strong and flexible machine learning model, and it is one of the most widely used for regression, outlier identification, and linear or nonlinear classification. SVM is especially effective in classifying complex datasets that are small to medium in size and are suitable for a variety of multi-class pattern recognition applications. The easiest way to introduce the concept behind SVM it's starting from its simplest form, the linear SVM. The algorithm divides the data into classes by generating a line if the feature space has two dimensions, a plane if the feature space has three dimensions, or a hyperplane if the feature space dimension is greater than three. When there are multiple hyperplanes for the same linear model, SVM searches for the one that offers the greatest margin. This means that it searches for the one that can maximise the distance between the hyperplane and the points from the various classes, that are closest to the hyperplane, known as support vectors, which results in a decrease in misclassification error. The further away the data are from the hyperplane, the higher the likelihood of correctly classifying the points [73], [74].

To better understand, it's possible to define the dataset like *n* vectors x_i. Each x_i will also be associated with a value y_i, the label, indicating if the element belongs to the class or not, so that can only have two possible values -1 or +1 [75]. Any hyperplane can be now defined as a set of points x_i satisfying:

$$\vec{w}x + b = 0$$

(32)

where *w* is a weight vector associated to *x*, the input feature vector, and *b* is the bias. Considering a feature space dimension equal to *n*, the hyperplane equation becomes:

$$b + w_1 x_1 + w_2 x_2 + \cdots w_n x_n = 0$$

(33)

In other terms, a linear combination of all dimensions equal to zero defines a hyperplane. Considering instead a binary classification [75], and including margin borders conditions, it's possible to regulate w_1 and w_2 as follows:

$$b + w_1 x_1 + w_2 x_2 \geq 0 \quad for\ y = +1$$

(34)

$$b + w_1 x_1 + w_2 x_2 \leq 0 \quad for\ y = -1$$

Now if *w* represents weights vector and $\|w\|$ is its length, we have that the maximal dimension of margin is:

$$\frac{1}{|w|} + \frac{1}{|w|} = \frac{2}{|w|}$$

(35)

The goal is to maximize the margin. Among all possible hyperplanes meeting the constraints, it will be chosen the hyperplane with the smallest $\|w\|$ because it is the one which will have the biggest margin [75]. So, minimizing the weight vector *w*, it's obtained the maximal margin, hence, the optimal hyperplane, as shown in figure 18.

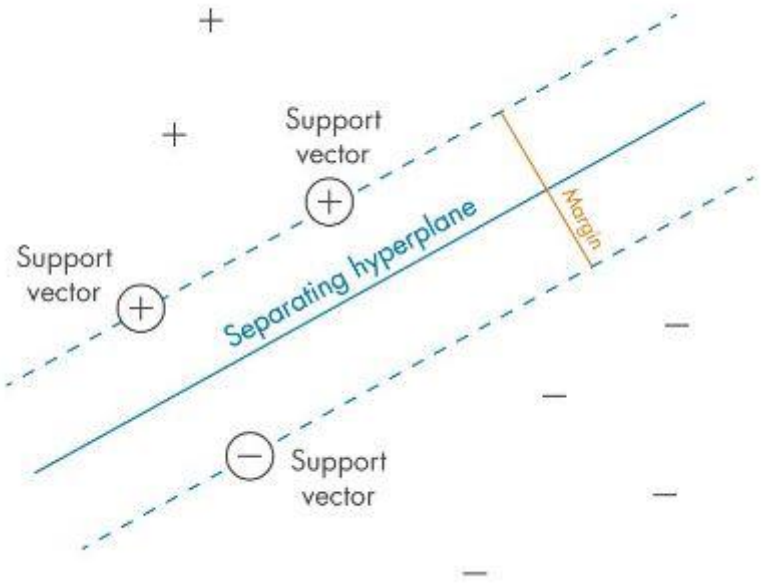

Figure 18: Definition of the margin between classes (here represented with + and -) the criterion that SVMs try to optimize [76].

Although linear SVM classifiers are efficient and work well in many cases, many datasets are not even close to being linearly separable [73]. If the algorithms are unable to locate such a hyperplane, training data is transformed into a higher dimension via a non-linear mapping. Thus, when data are

not linearly separable, a kernel technique is utilised. This method essentially seeks to transform the original data into a higher-dimensional linearly separable data set. Without entirely altering the input, a non-linear classifier can be created by utilising a non-linear kernel.

There are various kernel types, like a polynomial kernel of second order or a gaussian radial basis function (RBF) kernel [76]. The performance of the SVM model can be significantly impacted by the kernel function selected. For the pattern recognition purpose of the current study, it was selected the gaussian kernel, reported in the equation:

$$G(x_1, x_2) = \exp(-\|x_1 - x_2\|^2) \tag{36}$$

2.9.4 K-Nearest Neighbours

The KNN technique is the last machine learning algorithm chosen in this thesis since it is a common approach used in the literature to deal with pattern recognition from myoelectric data, and because it's simple and easy to implement. The basic concept behind it is very intuitive. Starting from a set *X* of *n* points, KNN tries to find the *k* closest points in *X* to a query point or set of points *Y* [73]. Starting from the assumption that similar inputs have similar outputs, in KNN classification, the output is a class membership. An object is classified by a plurality vote of its neighbours, with the object being assigned to the class most common among its *k* nearest neighbours, where *k* is a positive integer, as shown in figure 19. If $k = 1$, then the object is simply assigned to the class of that single nearest neighbour [77].

The KNN method for classifying objects is, in simple words, based on learning data of which the closest distance to the object. In contrast to regression, which focuses on the number value a variable will have, classification refers to an attempt to determine whether a given case will fall into a particular category or class. [78]. The distance of the neighbours in learning the KNN method is usually calculated based on Euclidean distance. Therefore, the regulation and policy should be considered first before the implementation takes place due to decision point leading to quality of the result as well as effectiveness and efficiency [77], [79]. In fact, there are a lot of other formulas that can be applied for the calculation of the distance of the neighbours depending on the circumstances, such as the Hamming distance, the Manhattan distance, or the Minkowski distance.

For the purpose of this work, the Euclidean distance formulation have been chosen, which is a measure of the true straight-line distance between two points in the Euclidean space:

$$d(x,y) = \sqrt{\sum_{i=1}^{n}(x_i - y_i)^2}$$

(37)

Where x_i and y_i stand for the two generic points between which the distance is determined each time, up until all n points have been taken into account. The disadvantage of this Euclidean distance function is that if one attribute input has a relatively large range, it can defeat other attributes. Consequently, distance is often normalized by dividing the distance for each attribute with the range, the maximum value minus minimum value, of the attribute so that the values for each attribute have a normalized new range of 0 to 1 [77]:

$$y = \frac{x - x_{min}}{x_{max} - x_{min}}$$

(38)

Where x is the value of the data, y is the value of the normalization and x_{max}, x_{min} are respectively minimum and maximum value.

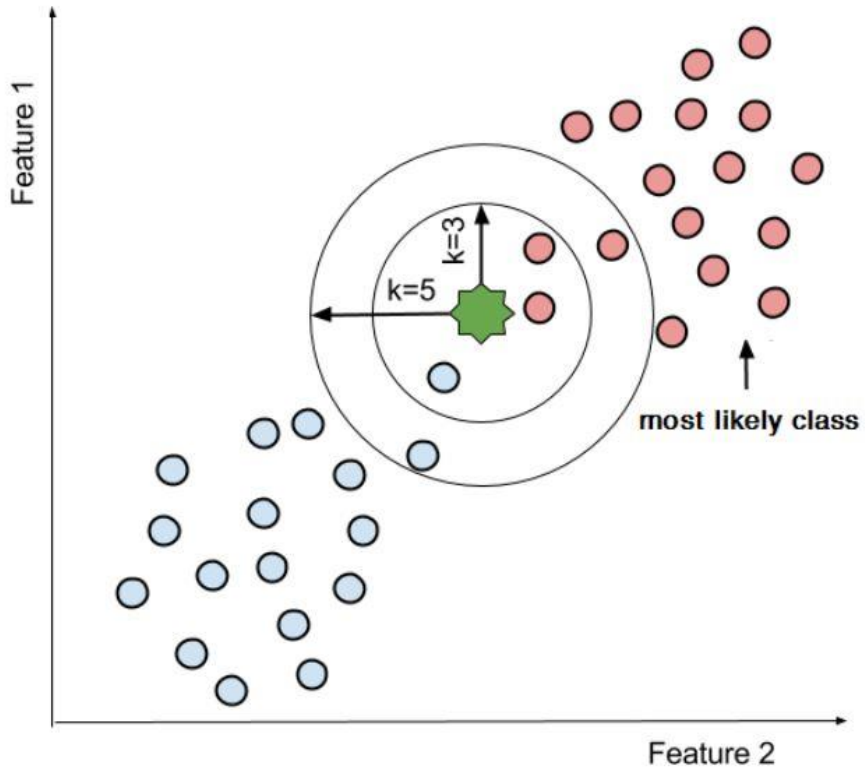

Figure 19: A typical example of a KNN classification for a two-class problem (i.e. the "pink" and the "blue" circles) when the *k* parameter is set to "3" and "5". The green star represents the sample point that needs to be classified [80].

2.10 Classifier performance metrics

In order to evaluate the performance of the machine learning classifiers considered, six classical metrics [81] have been taken into account: the accuracy, the precision, the recall, the specificity, the F1 score and the Matthews correlation coefficient. All of them are based on the performance of the algorithm after the testing phase, related to the actual classes and the predicted classes, coming from a specific table layout, that allows visualization of the performance of an algorithm, the confusion matrix, shown in figure 20 [82]. This is expressed in terms of true positive (TP), which corresponds to all the elements that have been correctly classified, true negative (TN), which corresponds to where the model correctly predicted the negative class, the false positive (FP) and false negative (FN) that are, respectively, the outcome where the model incorrectly predicted the positive or the negative classes.

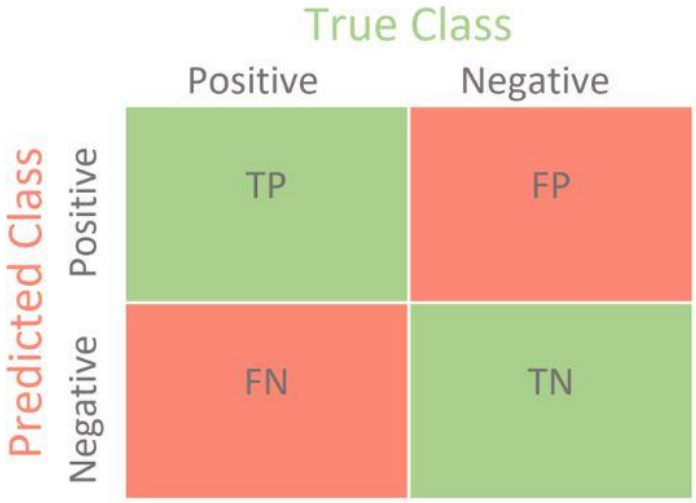

Figure 20: Confusion Matrix for Binary Classification [82].

The six meters evaluated are now briefly introduced [81].

- In classification problems, the accuracy is the fraction of accurate predictions made by the model among all possible predictions. This measure should be used when the target variable classes in the data are fairly balanced. Since in the dataset considered in this study there are an equal number of samples situation that belong to each class and no class predominates over the others, the accuracy is a reliable metric. It is defined as:

$$Accuracy = \frac{Number\ of\ correct\ predictions}{Total\ number\ of\ predictions\ made} =$$

(39)

$$= \frac{TP + TN}{TP + TN + FP + FN}$$

- The precision measures the proportion of predicted positive classes that actually fall into the positive class:

$$Precision = \frac{TP}{TP + FP}$$

(40)

- The fraction of negative data points that are accurately interpreted as negative, relative to all negative data points, is known as specificity, or true negative rate:

$$Specificity = \frac{TN}{TN + FP}$$

(41)

- The percentage of positive data points that are accurately interpreted as positive, relative to all positive data points, is known as recall or sensitivity and can be expressed as:

$$Recall = \frac{TP}{FN + TP}$$

(42)

- The F1 score is the harmonic mean between recall and precision. This statistic measures the classifier's accuracy, so the proportion of cases that it correctly categorises, and robustness, the proportion of instances it does not miss. The F1 Score determines how well the model performs and for this reason it's one of the most important metrics; the higher the F1 Score, the better the model works. In formulas it is:

$$F1 = 2\frac{precision\ recall}{precision + recall}$$

(43)

- As an alternative measure unaffected by the unbalanced datasets issue, the Matthews correlation coefficient (MCC) is a statistical tool used for model evaluation. Its task is to gauge or measure the difference between the predicted values and actual values. MCC is a best single-value classification metric which helps to summarize the confusion matrix or an error matrix. If the prediction returns good rates for all four of these entities, it is said to be a reliable measure producing high scores. To suit most correlation coefficients, MCC ranges between

+1 and -1 as: +1 is the best agreement between the predicted and actual values and 0 is no agreement. Mathematically, it can be expressed as:

$$MCC = \frac{TP \cdot TN - FP \cdot FN}{\sqrt{(TP + FP) \cdot (TP + FN) \cdot (TN + FP) \cdot (TN + FN)}} \tag{44}$$

2.10.1 Majority voting

Once the selected models have been applied using the previously described parameters, a further step has been taken. This is the majority voting, performed on the output of each model. As small window sizes can produce large classification errors, a post-processing approach, called majority voting (MV), is normally used to enhance the models' performances, and widely adopted for real time applications [83], [84]. MV utilizes a high-density stream of class decisions that resulted from the sliding window with an overlapping scheme to smooth out any potential noisy decision [85], [86]. In order to increase stability and robustness of the class decision stream, MV stipulates that the output of the classifier is not simply the most recent class decision but the class that appears the most often in the previous *n* class decisions [87]. The number of decisions used in the MV is determined by the processing time, the time consumed during feature extraction, projection and classification, and the acceptable delay which is the response time of the control system [88]. As regards the purposes of this study, the majority voting procedure was adopted in post-processing for all three chosen methods [89] and *n* was set to 4. To explain it simply, the majority voting was applied to the model output, so to the class label predicted. After that, it's again considered a window of data to count the number of votes for each class, find the class with the most votes and thus eliminate each spurious classification, combining it with the class most present in the surroundings. As a next step, in order to evaluate the real improvements obtained, the six classifier performance metrics were again considered and compared, in each of all the sub-cases examined, with the results obtained before the application of majority voting.

A further comparison among all the outputs obtained was then performed through the Wilcoxon rank sum test [90] (a nonparametric test for two populations when samples are independent [91]). This step allowed to understand if the differences among the performances obtained from the cases analysed, could be considered statistically significant (with a p-value<0.05) or not.

3 Results

The results can be divided according to the specific aspect from which they originate: it's possible to start considering the difference between the classification algorithms' performances when the whole electrodes setup and the globality of the features are considered. A second section it's dedicated to the SVM, LDA and KNN performances when the five feature sets are taken into account and when the electrodes are considered all together or making a distinction between forearm and wrist. The third section shows the same cases for the inter subject analysis, where the features extracted coming from the six subjects are concatenated and analysed as a whole. The last section reports the results obtained through the use of the MV in all the cases.

3.1 Classifier performances

This section is dedicated to the difference between the three classification algorithms' performances, when considering all the six electrodes and all the 27 features. In Table 3, 4 and 5 are reported the values of the performance metrics, respectively for the KNN, the SVM and LDA. Classifiers' performances are reported as the average between the six participants. In Figure 21, 22, 23 are shown the confusion matrices, coming from the analysis of one subject.

Scores KNN, six electrodes

ACC	AvgACC	PREC	RECALL	SPEC	F1	MCC	
0.82	0.99	0.83	0.82	0.99	0.82	0.82	**sub 1**
0.87	0.99	0.88	0.87	0.99	0.87	0.87	**sub 2**
0.85	0.99	0.85	0.85	0.99	0.85	0.84	**sub 3**
0.86	0.99	0.86	0.85	0.99	0.86	0.85	**sub 4**
0.83	0.99	0.84	0.83	0.99	0.83	0.83	**sub 5**
0.88	0.99	0.88	0.88	0.99	0.88	0.88	**sub 6**
0.85	0.99	0.86	0.85	0.99	0.85	0.85	**mean**

Table 3: Performance metrics of the KNN for all the subjects; the mean value between all the subjects it's also indicated.

Scores SVM, six electrodes

ACC	AvgACC	PREC	RECALL	SPEC	F1	MCC	
0.64	0.96	0.66	0.64	0.98	0.65	0.62	**sub 1**
0.66	0.97	0.70	0.66	0.98	0.68	0.64	**sub 2**
0.60	0.96	0.62	0.60	0.98	0.61	0.58	**sub 3**
0.63	0.96	0.64	0.63	0.98	0.63	0.61	**sub 4**
0.63	0.96	0.65	0.63	0.98	0.64	0.62	**sub 5**
0.688	0.97	0.69	0.68	0.98	0.68	0.66	**sub 6**
0.64	0.96	0.66	0.64	0.98	0.65	0.62	**mean**

Table 4: Performance metrics of the SVM for all the subjects; the mean value between all the subjects it's also indicated.

Scores LDA, six electrodes

ACC	AvgACC	PREC	RECALL	SPEC	F1	MCC	
0.37	0.89	0.39	0.37	0.94	0.38	0.32	**sub 1**
0.33	0.88	0.33	0.33	0.93	0.33	0.26	**sub 2**
0.31	0.87	0.31	0.31	0.93	0.31	0.23	**sub 3**
0.39	0.91	0.42	0.39	0.95	0.41	0.35	**sub 4**
0.38	0.90	0.39	0.38	0.95	0.39	0.33	**sub 5**
0.42	0.92	0.43	0.42	0.95	0.42	0.38	**sub 6**
0.37	0.89	0.38	0.37	0.94	0.37	0.31	**mean**

Table 5: Performance metrics of the LDA for all the subjects; the mean value between all the subjects it's also indicated.

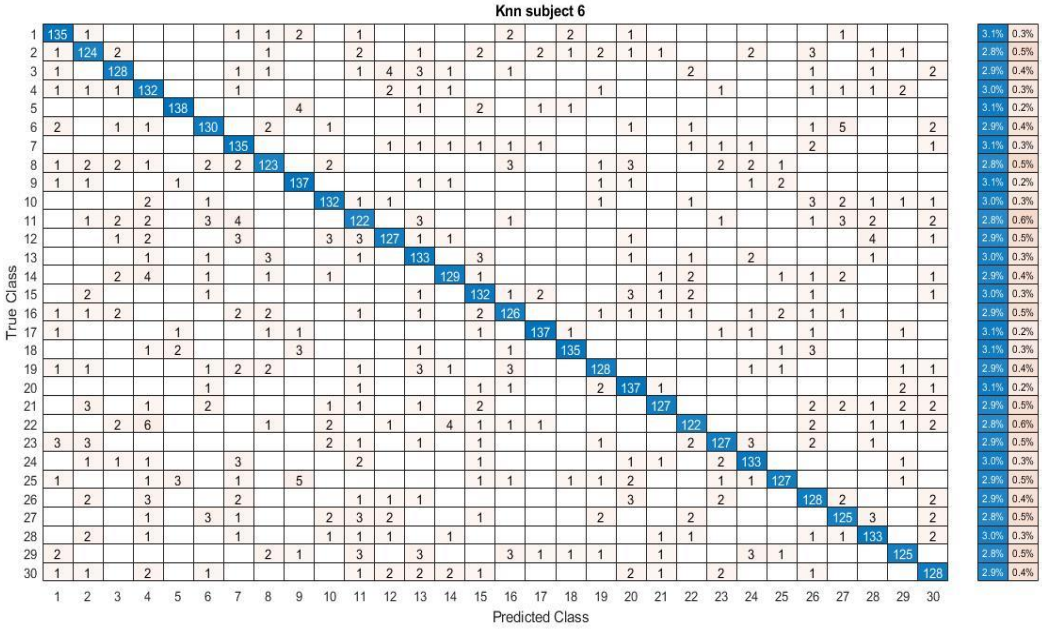

Figure 21: Confusion matrix from KNN classifier in the case of the subject number six.

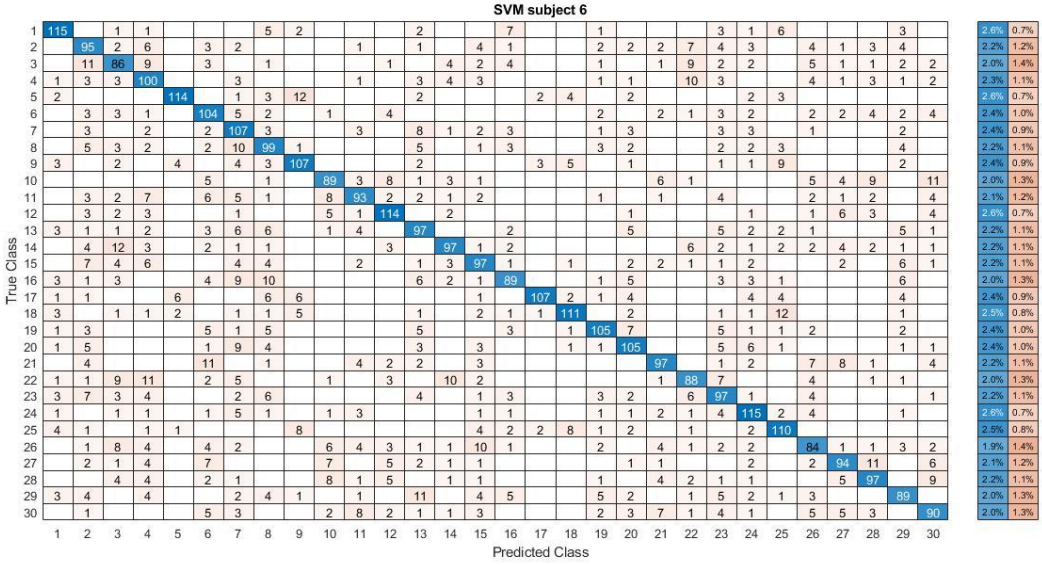

Figure 22: Confusion matrix from SVM classifier in the case of the subject number six.

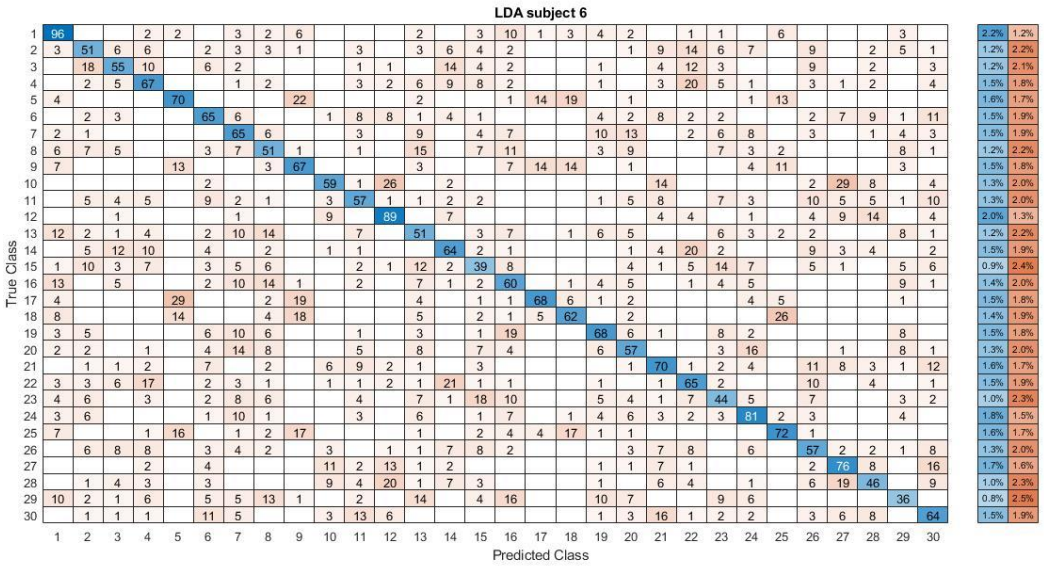

Figure 23: Confusion matrix from LDA classifier in the case of the subject number six.

3.2 Feature sets performances

This section it's dedicated to the SVM, LDA and KNN performances when the five feature sets are taken into account. Five tables are reported (Table 6-10) with the values of the performance metrics for the KNN, the SVM and the LDA, when all the electrodes are considered in the specific feature sets. Also in this case, the average value of the classification performances among the six participants is reported.

Hudgins feature set

Scores KNN							
ACC	**AvgACC**	**PREC**	**RECALL**	**SPEC**	**F1**	**MCC**	
0.60	0.96	0.61	0.60	0.98	0.60	0.58	**sub 1**
0.63	0.96	0.64	0.63	0.98	0.64	0.62	**sub 2**
0.59	0.96	0.59	0.59	0.98	0.59	0.57	**sub 3**
0.61	0.96	0.61	0.61	0.98	0.61	0.59	**sub 4**
0.55	0.95	0.56	0.55	0.97	0.55	0.52	**sub 5**
0.66	0.97	0.66	0.66	0.98	0.66	0.64	**sub 6**
0.61	0.96	0.61	0.61	0.98	0.61	0.59	**mean**
Scores SVM							
ACC	**AvgACC**	**PREC**	**RECALL**	**SPEC**	**F1**	**MCC**	

0.29	0.86	0.32	0.29	0.92	0.30	0.20	**sub 1**
0.26	0.84	0.26	0.26	0.91	0.26	0.17	**sub 2**
0.25	0.83	0.25	0.25	0.91	0.25	0.16	**sub 3**
0.30	0.87	0.31	0.30	0.92	0.31	0.23	**sub 4**
0.29	0.86	0.29	0.29	0.92	0.29	0.21	**sub 5**
0.36	0.89	0.36	0.36	0.94	0.36	0.29	**sub 6**
0.29	0.86	0.30	0.29	0.92	0.29	0.21	**mean**
Scores LDA							
ACC	**AvgACC**	**PREC**	**RECALL**	**SPEC**	**F1**	**MCC**	
0.23	0.82	0.24	0.23	0.90	0.24	0.13	**sub 1**
0.20	0.79	0.18	0.20	0.88	0.19	0.08	**sub 2**
0.20	0.79	0.18	0.20	0.88	0.19	0.09	**sub 3**
0.24	0.83	0.25	0.24	0.90	0.25	0.14	**sub 4**
0.24	0.82	0.23	0.24	0.90	0.23	0.15	**sub 5**
0.29	0.86	0.29	0.29	0.92	0.29	0.22	**sub 6**
0.23	0.82	0.23	0.23	0.89	0.23	0.14	**mean**

Table 6: Performance metrics of the KNN, SVM and LDA in the case of Hudgins feature set. All the subjects and the mean value between them it's also indicated.

Du feature set

Scores KNN							
ACC	**AvgACC**	**PREC**	**RECALL**	**SPEC**	**F1**	**MCC**	
0.64	0.96	0.64	0.64	0.98	0.64	0.62	**sub 1**
0.65	0.96	0.65	0.65	0.98	0.65	0.63	**sub 2**
0.62	0.96	0.62	0.62	0.97	0.62	0.60	**sub 3**
0.61	0.96	0.62	0.61	0.97	0.62	0.59	**sub 4**
0.58	0.95	0.58	0.58	0.97	0.58	0.56	**sub 5**
0.67	0.96	0.67	0.67	0.98	0.67	0.65	**sub 6**
0.63	0.96	0.63	0.63	0.98	0.63	0.61	**mean**
Scores SVM							
ACC	**AvgACC**	**PREC**	**RECALL**	**SPEC**	**F1**	**MCC**	
0.29	0.86	0.31	0.29	0.92	0.30	0.20	**sub 1**

0.25	0.84	0.26	0.25	0.91	0.26	0.17	**sub 2**
0.26	0.84	0.25	0.26	0.91	0.25	0.17	**sub 3**
0.32	0.88	0.33	0.32	0.93	0.33	0.26	**sub 4**
0.30	0.86	0.31	0.30	0.92	0.30	0.23	**sub 5**
0.37	0.89	0.37	0.37	0.94	0.37	0.31	**sub 6**
0.30	0.86	0.31	0.30	0.92	0.30	0.22	**mean**
Scores LDA							
ACC	**AvgACC**	**PREC**	**RECALL**	**SPEC**	**F1**	**MCC**	
0.26	0.84	0.26	0.26	0.91	0.26	0.17	**sub 1**
0.21	0.80	0.21	0.21	0.89	0.21	0.11	**sub 2**
0.22	0.81	0.21	0.22	0.89	0.21	0.13	**sub 3**
0.28	0.85	0.29	0.28	0.91	0.28	0.20	**sub 4**
0.27	0.85	0.27	0.27	0.91	0.27	0.20	**sub 5**
0.31	0.87	0.31	0.31	0.93	0.31	0.25	**sub 6**
0.26	0.84	0.26	0.26	0.91	0.26	0.18	**mean**

Table 7: Performance metrics of the KNN, SVM and LDA in the case of Du feature set. All the subjects and the mean value between them it's also indicated.

Phinyomark feature set 1

Scores KNN							
ACC	**AvgACC**	**PREC**	**RECALL**	**SPEC**	**F1**	**MCC**	
0.70	0.97	0.70	0.70	0.98	0.70	0.68	**sub 1**
0.76	0.98	0.77	0.76	0.98	0.76	0.75	**sub 2**
0.69	0.97	0.69	0.69	0.98	0.69	0.68	**sub 3**
0.73	0.97	0.73	0.73	0.98	0.73	0.71	**sub 4**
0.72	0.97	0.72	0.72	0.98	0.72	0.70	**sub 5**
0.78	0.98	0.78	0.78	0.99	0.78	0.77	**sub 6**
0.73	0.97	0.73	0.73	0.98	0.73	0.72	**mean**
Scores SVM							
ACC	**AvgACC**	**PREC**	**RECALL**	**SPEC**	**F1**	**MCC**	
0.38	0.90	0.40	0.38	0.94	0.39	0.32	**sub 1**
0.39	0.90	0.40	0.39	0.949	0.39	0.33	**sub 2**

0.35	0.89	0.35	0.35	0.94	0.35	0.29	**sub 3**
0.41	0.91	0.41	0.41	0.95	0.41	0.36	**sub 4**
0.39	0.90	0.39	0.39	0.94	0.39	0.34	**sub 5**
0.49	0.93	0.49	0.49	0.96	0.49	0.45	**sub 6**
0.40	0.90	0.41	0.40	0.95	0.40	0.35	**mean**
Scores LDA							
ACC	**AvgACC**	**PREC**	**RECALL**	**SPEC**	**F1**	**MCC**	
0.27	0.85	0.28	0.27	0.91	0.27	0.19	**sub 1**
0.25	0.83	0.24	0.25	0.90	0.25	0.16	**sub 2**
0.25	0.83	0.24	0.25	0.91	0.25	0.17	**sub 3**
0.31	0.87	0.32	0.31	0.93	0.32	0.24	**sub 4**
0.29	0.86	0.28	0.29	0.92	0.28	0.22	**sub 5**
0.34	0.88	0.34	0.34	0.93	0.34	0.28	**sub 6**
0.28	0.85	0.28	0.28	0.92	0.28	0.21	**mean**

Table 8: Performance metrics of the KNN, SVM and LDA in the case of Phinyomark feature set 1. All the subjects and the mean value between them it's also indicated.

Phinyomark feature set 2

Scores KNN							
ACC	**AvgACC**	**PREC**	**RECALL**	**SPEC**	**F1**	**MCC**	
0.64	0.96	0.65	0.64	0.98	0.65	0.63	**sub 1**
0.692	0.97	0.69	0.69	0.98	0.69	0.67	**sub 2**
0.60	0.95	0.60	0.60	0.97	0.60	0.58	**sub 3**
0.62	0.96	0.62	0.62	0.97	0.62	0.60	**sub 4**
0.64	0.96	0.64	0.64	0.98	0.64	0.62	**sub 5**
0.72	0.97	0.72	0.72	0.98	0.72	0.70	**sub 6**
0.65	0.96	0.65	0.65	0.98	0.65	0.63	**mean**
Scores SVM							
ACC	**AvgACC**	**PREC**	**RECALL**	**SPEC**	**F1**	**MCC**	
0.33	0.88	0.36	0.33	0.93	0.34	0.27	**sub 1**
0.32	0.87	0.33	0.32	0.93	0.32	0.24	**sub 2**
0.29	0.86	0.30	0.29	0.92	0.29	0.21	**sub 3**
0.36	0.89	0.37	0.36	0.94	0.37	0.30	**sub 4**

0.34	0.88	0.35	0.34	0.93	0.35	0.28	**sub 5**
0.40	0.90	0.41	0.40	0.95	0.40	0.34	**sub 6**
0.34	0.88	0.35	0.34	0.93	0.35	0.27	**mean**
Scores LDA							
ACC	**AvgACC**	**PREC**	**RECALL**	**SPEC**	**F1**	**MCC**	
0.28	0.85	0.28	0.28	0.91	0.28	0.19	**sub 1**
0.23	0.82	0.22	0.23	0.89	0.23	0.13	**sub 2**
0.23	0.82	0.22	0.23	0.89	0.23	0.14	**sub 3**
0.28	0.85	0.30	0.28	0.92	0.29	0.20	**sub 4**
0.28	0.85	0.27	0.28	0.92	0.27	0.21	**sub 5**
0.31	0.87	0.31	0.31	0.92	0.31	0.24	**sub 6**
0.27	0.84	0.27	0.27	0.91	0.27	0.18	**mean**

Table 9: Performance metrics of the KNN, SVM and LDA in the case of Phinyomark feature set 2. All the subjects and the mean value between them it's also indicated.

TDAR feature set

Scores KNN							
ACC	**AvgACC**	**PREC**	**RECALL**	**SPEC**	**F1**	**MCC**	
0.72	0.97	0.73	0.72	0.98	0.72	0.71	**sub 1**
0.78	0.98	0.78	0.78	0.99	0.78	0.77	**sub 2**
0.70	0.97	0.70	0.70	0.98	0.70	0.69	**sub 3**
0.73	0.97	0.73	0.73	0.98	0.73	0.72	**sub 4**
0.72	0.97	0.72	0.72	0.98	0.72	0.70	**sub 5**
0.80	0.98	0.80	0.80	0.99	0.80	0.79	**sub 6**
0.74	0.97	0.74	0.74	0.98	0.74	0.73	**mean**
Scores SVM							
ACC	**AvgACC**	**PREC**	**RECALL**	**SPEC**	**F1**	**MCC**	
0.37	0.90	0.39	0.37	0.94	0.38	0.31	**sub 1**
0.37	0.89	0.38	0.37	0.94	0.37	0.31	**sub 2**
0.33	0.88	0.33	0.33	0.93	0.33	0.269	**sub 3**
0.41	0.91	0.42	0.41	0.95	0.41	0.36	**sub 4**

0.38	0.90	0.39	0.38	0.94	0.39	0.33	**sub 5**
0.47	0.93	0.48	0.47	0.96	0.48	0.44	**sub 6**
0.39	0.90	0.40	0.39	0.94	0.39	0.33	**mean**
Scores LDA							
ACC	**AvgACC**	**PREC**	**RECALL**	**SPEC**	**F1**	**MCC**	
0.27	0.85	0.28	0.27	0.91	0.28	0.19	**sub 1**
0.24	0.82	0.23	0.24	0.90	0.23	0.14	**sub 2**
0.25	0.83	0.25	0.25	0.91	0.25	0.17	**sub 3**
0.31	0.87	0.32	0.31	0.93	0.32	0.24	**sub 4**
0.30	0.86	0.29	0.30	0.92	0.29	0.23	**sub 5**
0.34	0.88	0.34	0.34	0.93	0.34	0.28	**sub 6**
0.29	0.85	0.29	0.29	0.92	0.29	0.21	**mean**

Table 10: Performance metrics of the KNN, SVM and LDA in the case of TDAR feature set. All the subjects and the mean value between them it's also indicated.

3.2.1 Reduced electrodes setup

In this section are reported the SVM, LDA and KNN performances when the five feature sets are considered and there is the distinction between the four forearm electrodes and the two wrist electrodes. Five tables (Table 11-15) are reported, with the average values for the classification performances computed among the entire population.

Hudgins feature set

	ACC	**AvgACC**	**PREC**	**RECALL**	**SPEC**	**F1**	**MCC**
KNN, F	0.37	0.89	0.37	0.37	0.94	0.37	0.31
KNN,W	0.11	0.66	0.11	0.11	0.79	0.11	-0.09
SVM, F	0.21	0.79	0.21	0.21	0.88	0.21	0.09
SVM,W	0.10	0.65	0.11	0.10	0.79	0.11	-0.12
LDA, F	0.18	0.76	0.17	0.18	0.86	0.17	0.04
LDA,W	0.09	0.63	0.08	0.09	0.78	0.09	-0.14

Table 11: Hudgins feature set's performance metrics in the case of Knn, SVM and LDA. "F" stays for forearm electrodes, "W" stays for wrist electrodes. The mean among the metrics values obtained from the six subjects are reported.

Du feature set

	ACC	AvgACC	PREC	RECALL	SPEC	F1	MCC
KNN, F	0.41	0.91	0.41	0.41	0.95	0.41	0.36
KNN,W	0.13	0.69	0.13	0.13	0.81	0.13	-0.05
SVM, F	0.22	0.81	0.23	0.22	0.89	0.23	0.12
SVM,W	0.11	0.65	0.11	0.11	0.80	0.11	-0.11
LDA, F	0.20	0.78	0.19	0.20	0.87	0.19	0.08
LDA,W	0.10	0.64	0.09	0.10	0.78	0.09	-0.12

Table 12: Hudgins feature set's performance metrics in the case of KNN, SVM and LDA. "F" stays for forearm electrodes, "W" stays for wrist electrodes. The mean among the metrics values obtained from the six subjects are reported.

Phinyomark feature set 1

	ACC	AvgACC	PREC	RECALL	SPEC	F1	MCC
KNN, F	0.58	0.95	0.59	0.58	0.97	0.58	0.56
KNN,W	0.29	0.86	0.30	0.29	0.92	0.30	0.22
SVM, F	0.28	0.85	0.29	0.28	0.91	0.28	0.20
SVM,W	0.13	0.70	0.13	0.13	0.82	0.13	-0.04
LDA, F	0.22	0.80	0.21	0.22	0.89	0.22	0.11
LDA,W	0.12	0.68	0.11	0.12	0.80	0.11	-0.06

Table 13: Phinyomark first feature set's performance metrics in the case of KNN, SVM and LDA. "F" stays for forearm electrodes, "W" stays for wrist electrodes. The mean among the metrics values obtained from the six subjects are reported.

Phinyomark feature set 2

	ACC	AvgACC	PREC	RECALL	SPEC	F1	MCC
KNN, F	0.49	0.93	0.50	0.49	0.96	0.50	0.46

KNN,W	0.23	0.82	0.23	0.23	0.90	0.23	0.13
SVM, F	0.24	0.82	0.25	0.24	0.90	0.24	0.13
SVM,W	0.12	0.69	0.12	0.12	0.81	0.12	-0.06
LDA, F	0.20	0.79	0.20	0.20	0.88	0.20	0.08
LDA,W	0.11	0.66	0.10	0.11	0.80	0.10	-0.08

Table 14: Phinyomark second feature set's performance metrics in the case of KNN, SVM and LDA. "F" stays for forearm electrodes, "W" stays for wrist electrodes. The mean among the metrics values obtained from the six subjects are reported.

TDAR feature set

	ACC	**AvgACC**	**PREC**	**RECALL**	**SPEC**	**F1**	**MCC**
KNN, F	0.59	0.95	0.59	0.59	0.97	0.59	0.56
KNN,W	0.28	0.85	0.28	0.28	0.91	0.28	0.20
SVM, F	0.27	0.84	0.27	0.27	0.91	0.27	0.18
SVM,W	0.13	0.70	0.13	0.13	0.82	0.13	-0.05
LDA, F	0.22	0.80	0.22	0.22	0.89	0.22	0.11
LDA,W	0.12	0.68	0.11	0.12	0.80	0.11	-0.06

Table 15: TDAR feature set's performance metrics in the case of KNN, SVM and LDA. "F" stays for forearm electrodes, "W" stays for wrist electrodes. The mean among the metrics values obtained from the six subjects are reported.

3.3 Inter subject classifier behaviour

In this section are reported the results coming from the features extracted from the six subjects that are concatenated to obtain a single data matrix. In Table16 are reported the values of the performance metrics, respectively for the KNN, and the LDA, when all the electrodes are considered. After that, in Table 17 and 18 are shown the values of the classifiers' performance metrics in the five feature sets considered respectively when all the electrodes are considered and when the distinction between the four forearm electrodes and the two wrist electrodes is done.

Performance metrics, six electrodes

	ACC	AvgACC	PREC	RECALL	SPEC	F1	MCC
KNN	0.82	0.98	0.82	0.82	0.99	0.82	0.82
LDA	0.16	0.74	0.15	0.16	0.85	0.16	0.02

Table 16: KNN and LDA performance metrics when all the electrodes are considered. All the feature extracted from the six subjects are concatenated and considered together.

Feature sets performances, all the electrodes

		ACC	AvgACC	PREC	RECALL	SPEC	F1	MCC
Hudgins	KNN	0.53	0.94	0.53	0.53	0.97	0.53	0.50
	LDA	0.08	0.57	0.07	0.08	0.73	0.07	-0.20
Du	KNN	0.55	0.94	0.55	0.55	0.97	0.55	0.52
	LDA	0.08	0.58	0.07	0.08	0.74	0.08	-0.18
Phinyomark 1	KNN	0.67	0.96	0.67	0.67	0.98	0.67	0.66
	LDA	0.10	0.63	0.09	0.10	0.77	0.10	-0.12
Phinyomark 2	KNN	0.57	0.95	0.57	0.57	0.97	0.57	0.54
	LDA	0.08	0.59	0.08	0.08	0.74	0.08	-0.17
TDAR	KNN	0.68	0.96	0.68	0.68	0.98	0.68	0.66
	LDA	0.09	0.62	0.09	0.09	0.76	0.09	-0.14

Table 17: Values of the classifiers' performance metrics in the five feature sets when all the electrodes are considered.

Feature sets performances, forearm and wrist

Hudgins						
	ACC	AvgACC	PREC	RECALL	SPEC	F1	MCC
KNN, F	0.30	0.86	0.30	0.30	0.92	0.30	0.22
KNN,W	0.07	0.55	0.07	0.07	0.70	0.07	-0.21
LDA. F	0.07	0.54	0.06	0.07	0.71	0.06	-0.25
LDA,W	0.04	0.45	0.05	0.04	0.65	0.05	-0.38
Du							

	ACC	AvgACC	PREC	RECALL	SPEC	F1	MCC
KNN, F	0.32	0.87	0.32	0.32	0.93	0.32	0.25
KNN,W	0.08	0.57	0.08	0.08	0.72	0.08	-0.19
LDA. F	0.07	0.56	0.07	0.07	0.72	0.07	-0.22
LDA,W	0.05	0.46	0.04	0.05	0.66	0.05	-0.36

Phinyomark 1							
	ACC	**AvgACC**	**PREC**	**RECALL**	**SPEC**	**F1**	**MCC**
KNN, F	0.50	0.93	0.50	0.50	0.96	0.50	0.47
KNN,W	0.23	0.81	0.23	0.23	0.89	0.23	0.12
LDA. F	0.08	0.59	0.08	0.08	0.74	0.08	-0.17
LDA,W	0.05	0.48	0.05	0.05	0.66	0.05	-0.31

Phinyomark 2							
	ACC	**AvgACC**	**PREC**	**RECALL**	**SPEC**	**F1**	**MCC**
KNN, F	0.41	0.91	0.41	0.41	0.95	0.41	0.36
KNN,W	0.17	0.76	0.17	0.17	0.86	0.17	0.03
LDA. F	0.07	0.55	0.07	0.07	0.71	0.07	-0.22
LDA,W	0.05	0.47	0.05	0.05	0.66	0.05	-0.33

TDAR							
	ACC	**AvgACC**	**PREC**	**RECALL**	**SPEC**	**F1**	**MCC**
KNN, F	0.51	0.94	0.51	0.51	0.96	0.51	0.47
KNN,W	0.20	0.79	0.20	0.20	0.88	0.20	0.08
LDA. F	0.08	0.58	0.08	0.08	0.74	0.08	-0.18
LDA,W	0.05	0.48	0.05	0.05	0.66	0.05	-0.31

Table 18: Feature sets' performance metrics in the case of KNN and LDA. "F" stays for forearm electrodes, "W" stays for wrist electrodes.

3.4 Effect of the majority voting

In this section are reported all the results previously listed with the only difference that the majority voting is applied. In Table 19 are reported the values of the performance metrics of the three classifiers, when all the six subjects and all the electrodes are considered. In Figure 24, 25, 26 are

shown the confusion matrixes, respectively of KNN, SVM, and LDA classifier, coming from the analysis of one representative subject when the MV is applied. Are then reported five tables (Table 20-24) where the different feature sets are considered with the cases where all the electrodes or the only forearm and wrist electrodes are considered. In Table 25 are reported the results of the MV application, coming from the inter subject analysis.

Performance metrics, six electrodes, majority voting

Scores KNN							
ACC	**AvgACC**	**PREC**	**RECALL**	**SPEC**	**F1**	**MCC**	
0.95	0.99	0.95	0.95	0.99	0.95	0.95	**sub 1**
0.96	0.99	0.96	0.96	0.99	0.96	0.95	**sub 2**
0.96	0.99	0.96	0.96	0.99	0.96	0.96	**sub 3**
0.97	0.99	0.97	0.97	0.99	0.97	0.97	**sub 4**
0.96	0.99	0.96	0.96	0.99	0.96	0.96	**sub 5**
0.97	0.99	0.97	0.97	0.99	0.97	0.97	**sub 6**
0.96	0.99	0.96	0.96	0.99	0.96	0.96	**mean**
Scores SVM							
ACC	**AvgACC**	**PREC**	**RECALL**	**SPEC**	**F1**	**MCC**	
0.82	0.98	0.84	0.82	0.99	0.83	0.81	**sub 1**
0.84	0.98	0.86	0.84	0.99	0.85	0.83	**sub 2**
0.77	0.98	0.80	0.77	0.99	0.79	0.76	**sub 3**
0.82	0.98	0.83	0.82	0.99	0.83	0.82	**sub 4**
0.82	0.98	0.84	0.82	0.99	0.83	0.81	**sub 5**
0.86	0.98	0.86	0.86	0.99	0.86	0.85	**sub 6**
0.82	0.98	0.84	0.82	0.99	0.83	0.82	**mean**
Scores LDA							
ACC	**AvgACC**	**PREC**	**RECALL**	**SPEC**	**F1**	**MCC**	
0.53	0.94	0.56	0.53	0.97	0.55	0.51	**sub 1**
0.46	0.92	0.48	0.46	0.96	0.47	0.43	**sub 2**
0.42	0.91	0.46	0.42	0.95	0.44	0.40	**sub 3**
0.55	0.94	0.58	0.55	0.97	0.57	0.53	**sub 4**
0.49	0.93	0.51	0.49	0.96	0.50	0.47	**sub 5**
0.59	0.95	0.61	0.59	0.97	0.60	0.58	**sub 6**
0.51	0.93	0.53	0.51	0.96	0.52	0.49	**mean**

Table 19: Performance metrics of the KNN, SVM and LDA for all the subjects when the majority voting is applied; the mean value between all the subjects it's also indicated.

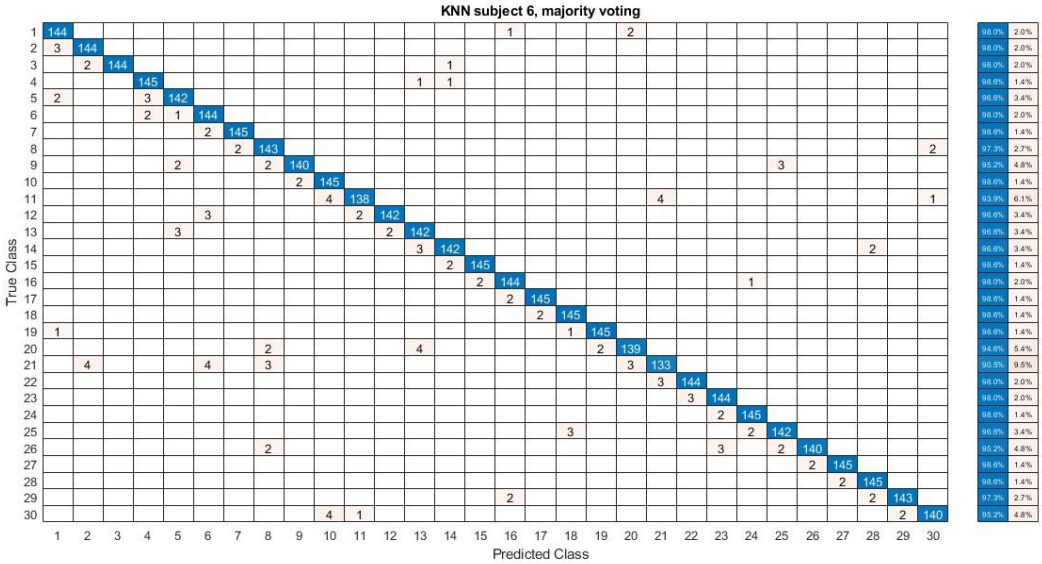

Figure 24: Confusion matrix from KNN classifier with the majority voting, in the case of the subject number six.

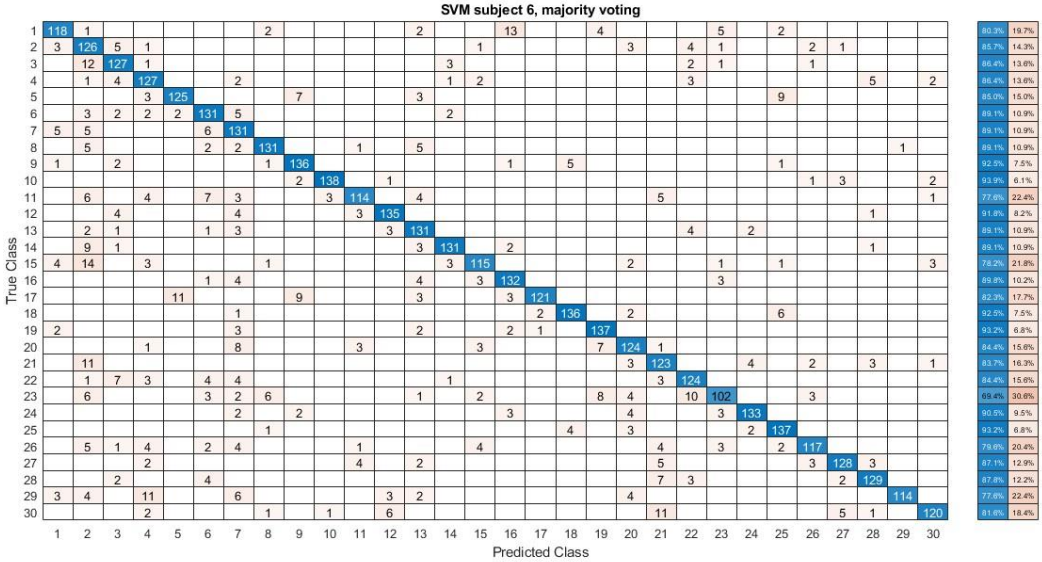

Figure 25: Confusion matrix from SVM classifier with the majority voting, in the case of the subject number six.

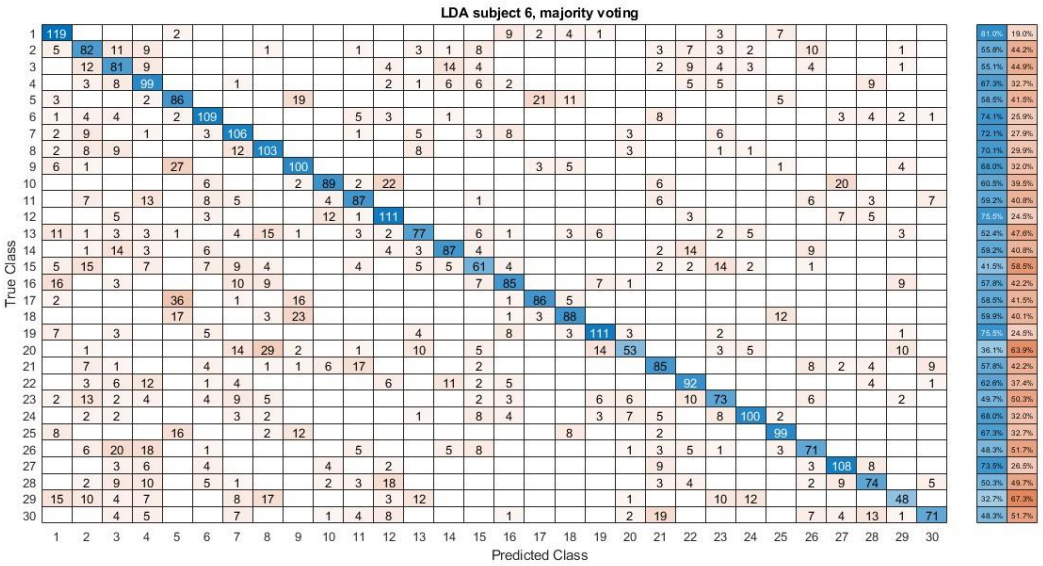

Figure 26: Confusion matrix from LDA classifier with the majority voting, in the case of the subject number six.

Hudgins feature set, majority voting

	ACC	AvgACC	PREC	RECALL	SPEC	F1	MCC
KNN, A	0.86	0.98	0.87	0.86	0.99	0.87	0.86
KNN,F	0.55	0.94	0.59	0.55	0.97	0.57	0.52
KNN,W	0.15	0.73	0.18	0.15	0.84	0.16	-0.01
SVM, A	0.21	0.79	0.21	0.21	0.88	0.21	0.09
SVM, F	0.25	0.83	0.27	0.25	0.90	0.26	0.17
SVM,W	0.13	0.71	0.15	0.13	0.84	0.14	-0.03
LDA, A	0.20	0.78	0.19	0.20	0.87	0.19	0.07
LDA, F	0.22	0.80	0.22	0.22	0.89	0.22	0.12
LDA,W	0.11	0.66	0.10	0.11	0.81	0.10	-0.08

Table 20: Hudgins feature set's performance metrics in the case of KNN, SVM and LDA. "A" stays for all the electrodes, "F" stays for forearm electrodes, "W" stays for wrist electrodes. The mean among the metrics values obtained from the six subjects are reported.

Du feature set, majority voting

	ACC	AvgACC	PREC	RECALL	SPEC	F1	MCC
KNN, A	0.88	0.99	0.88	0.88	0.99	0.88	0.87
KNN, F	0.63	0.96	0.68	0.63	0.98	0.65	0.62

KNN,W	0.18	0.77	0.22	0.18	0.87	0.19	0.04
SVM, A	0.40	0.90	0.42	0.40	0.95	0.41	0.36
SVM, F	0.28	0.85	0.30	0.28	0.91	0.29	0.20
SVM,W	0.12	0.69	0.13	0.12	0.83	0.12	-0.06
LDA, A	0.33	0.87	0.34	0.33	0.93	0.33	0.28
LDA, F	0.25	0.83	0.26	0.25	0.90	0.25	0.17
LDA,W	0.11	0.67	0.10	0.11	0.81	0.10	-0.08

Table 21: Du feature set's performance metrics in the case of KNN, SVM and LDA. "A" stays for all the electrodes, "F" stays for forearm electrodes, "W" stays for wrist electrodes. The mean among the metrics values obtained from the six subjects are reported.

Phinyomark feature set 1, majority voting

	ACC	**AvgACC**	**PREC**	**RECALL**	**SPEC**	**F1**	**MCC**
KNN, A	0.93	0.99	0.94	0.93	0.99	0.94	0.93
KNN, F	0.85	0.98	0.86	0.85	0.99	0.85	0.84
KNN,W	0.48	0.93	0.56	0.48	0.96	0.52	0.45
SVM, A	0.55	0.94	0.58	0.55	0.97	0.56	0.53
SVM, F	0.38	0.90	0.41	0.38	0.94	0.39	0.33
SVM,W	0.17	0.76	0.18	0.17	0.86	0.17	0.03
LDA, A	0.38	0.90	0.40	0.38	0.94	0.39	0.34
LDA, F	0.28	0.85	0.30	0.28	0.92	0.29	0.21
LDA,W	0.14	0.72	0.14	0.14	0.84	0.14	-0.03

Table 22: Phinyomark first feature set's performance metrics in the case of KNN, SVM and LDA. "A" stays for all the electrodes, "F" stays for forearm electrodes, "W" stays for wrist electrodes. The mean among the metrics values obtained from the six subjects are reported.

Phinyomark feature set 2, majority voting

	ACC	**AvgACC**	**PREC**	**RECALL**	**SPEC**	**F1**	**MCC**
KNN, A	0.90	0.99	0.90	0.90	0.99	0.90	0.89
KNN, F	0.76	0.97	0.79	0.76	0.98	0.77	0.75
KNN,W	0.37	0.89	0.44	0.37	0.94	0.40	0.31
SVM, A	0.46	0.92	0.49	0.46	0.96	0.48	0.43

SVM, F	0.32	0.87	0.35	0.32	0.93	0.33	0.26
SVM,W	0.15	0.74	0.15	0.15	0.85	0.15	0.01
LDA, A	0.34	0.88	0.35	0.34	0.93	0.35	0.29
LDA, F	0.26	0.83	0.27	0.26	0.91	0.26	0.19
LDA,W	0.13	0.71	0.12	0.13	0.83	0.13	-0.02

Table 23: Phinyomark second feature set's performance metrics in the case of KNN, SVM and LDA. "A" stays for all the electrodes, "F" stays for forearm electrodes, "W" stays for wrist electrodes. The mean among the metrics values obtained from the six subjects are reported.

TDAR feature set, majority voting

	ACC	**AvgACC**	**PREC**	**RECALL**	**SPEC**	**F1**	**MCC**
KNN, A	0.94	0.99	0.94	0.94	0.99	0.94	0.93
KNN, F	0.84	0.98	0.86	0.84	0.99	0.85	0.84
KNN,W	0.45	0.92	0.52	0.45	0.96	0.48	0.41
SVM, A	0.53	0.94	0.56	0.53	0.97	0.55	0.51
SVM, F	0.36	0.89	0.39	0.36	0.94	0.37	0.32
SVM,W	0.16	0.75	0.18	0.13	0.86	0.17	0.02
LDA, A	0.38	0.90	0.39	0.38	0.94	0.39	0.34
LDA, F	0.28	0.85	0.29	0.28	0.918015	0.28	0.21
LDA,W	0.14	0.72	0.13	0.14	0.84	0.14	-0.01

Table 24: TDAR second feature set's performance metrics in the case of KNN, SVM and LDA. "A" stays for all the electrodes, "F" stays for forearm electrodes, "W" stays for wrist electrodes. The mean among the metrics values obtained from the six subjects are reported.

All subjects, six electrodes, majority voting

		ACC	**AvgACC**	**PREC**	**RECALL**	**SPEC**	**F1**	**MCC**
Hudgins	KNN	0.79	0.98	0.81	0.7	0.99	0.80	0.78
	LDA	0.08	0.60	0.08	0.08	0.75	0.08	-0.18
Du	KNN	0.80	0.98	0.82	0.80	0.99	0.81	0.79
	LDA	0.09	0.62	0.09	0.09	0.77	0.09	-0.15

Phinyomark 1	KNN	0.92	0.99	0.92	0.92	0.99	0.92	0.91
	LDA	0.12	0.68	0.12	0.12	0.80	0.12	-0.08
Phinyomark 2	KNN	0.85	0.98	0.86	0.85	0.99	0.85	0.84
	LDA	0.09	0.63	0.09	0.09	0.77	0.09	-0.14
TDAR	KNN	0.92	0.99	0.92	0.92	0.99	0.92	0.91
	LDA	0.11	0.66	0.11	0.11	0.79	0.11	-0.10

Table 25: KNN and LDA performance metrics when all the electrodes are considered. All the feature extracted from the six subjects are concatenated and considered together, then the majority voting is performed.

4 Discussion and Conclusion

A first observation should be focused on the MV procedure in terms of real time processing delay. For the purpose of this study, it was decided to use only the previous *n* decisions (*n*=4 in this study) in the voting process without having to wait for future decisions. Thus, the system could still work within the real-time processing delay requirements [88]. The consideration of *n* future decisions could instead increase the processing delay limits beyond the optimal controller delay of 100-to-125 ms recommended in the literature [55].

4.1 Classifiers' performances

Recalling the tables 3, 4 and 5 and giving particular attention to the values of the metrics, it's obvious that the KNN is the learning model with the best performances. Furthermore, the confusion matrices reported in figure 21 shows how the elements have been correctly classified for most cases. Indeed, it can be seen how the diagonal contains most of the observations, even before the MV procedure (figure 24), where all the spurious misclassifications have been grouped. Comparing this with the confusion matrices of the SVM and the LDA algorithms (figure 22 and 23) it's possible to observe how the number of misclassified elements increase. The worst case it's obtained with the LDA classifier before and after the majority voting, as shown in the table 5 and 19. Among all the performance metrics, focusing on the accuracy, in figure 27 it's shown visually the difference among the three classifier algorithms, both before and after the majority voting. The KNN algorithm showed an average accuracy of 85.4%, before the majority voting, and making a comparison with the SVM accuracy (64.1%), even if the difference resulted to be not statistically significant (p=0.8832), the KNN showed higher performances with respect to SVM. The LDA, when performed without the majority voting, resulted with an inadequate classification accuracy (36.9%). When instead it is applied the majority voting, the LDA accuracy goes through an elevation until 51.2%, which confirms that the LDA can be considered not suitable for the purpose of this study.
In Table16 are reported the values of the performance metrics for the KNN and the LDA for the inter subject analysis. First of all, the KNN resulted to be the best classifier algorithm, even if the values of the performance metrics decreased as expected, but the important consideration in this case is that it was not possible to obtain results from the SVM because it is the most computational expensive

algorithm, among the three selected, and with the increase of the amount of the data, the SVM run become highly expensive in terms of computational demands.

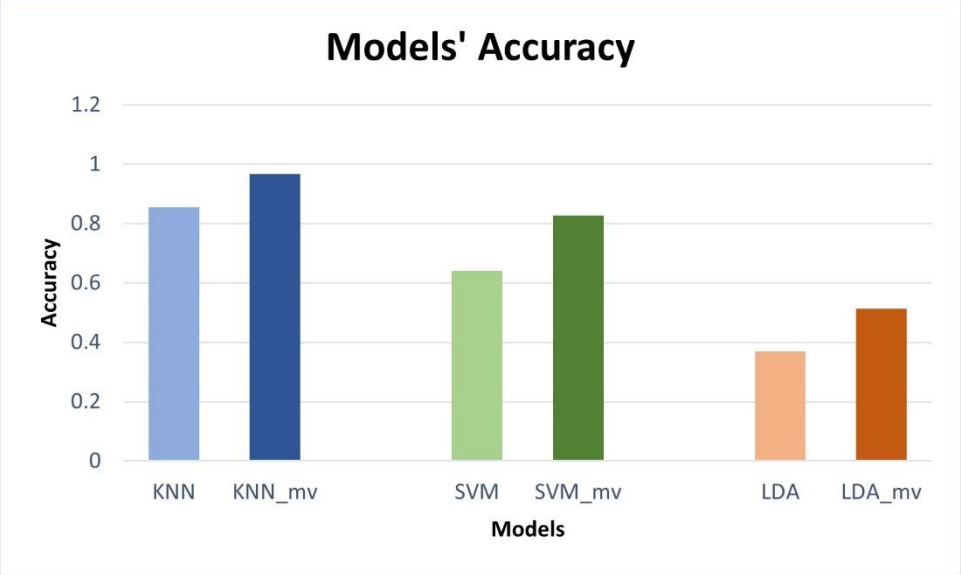

Figure 27: Bar plot of the accuracy of the KNN (in blue), SVM (in green), LDA (in orange) classifiers before and after the majority voting (indicated as "mv") is applied when the configuration of the six electrodes and the globality of the features are considered.

4.2 Feature sets analysis

In this study five common feature sets have been analysed. The KNN still resulted the one with the best performances among all the five feature sets explored, as reported in Table 6-10 from the *3.2 Feature sets performances* section, and the LDA algorithm resulted to have the worst performances. This scheme is confirmed also when the MV has been applied. Focusing again on the accuracy only (the same behaviour can be observed for the other performance metrics evaluated) and considering just the case of the KNN algorithm before the MV application, it's possible to make now a comparison between the five feature sets. Figure 28 wants to make possible to understand at first glance which shows the best accuracy. The best feature set turned out to be the TDAR, with an average accuracy of 74.6% without the MV, followed by the Phinyomark 1 feature set, with 73.4% of accuracy. From the statistical analysis it emerged that TDAR has a significant difference with respect to all the other feature sets, particularly with respect to Du feature set ($p=0.0022$), except for the Phinyomark 1 ($p=0.5887$). For what concern the Phinyomark 2 feature set, it still showed a statistical difference with respect TDAR ($p=0.0087$) and Phinyomark 1 ($p=0.0152$). All of those considerations regarding

the KNN can be extended to the other two classification algorithms, where again the best feature set in terms of performance metrics resulted to be the TDAR, even with poor performances (average accuracy of 39.3% for the SVM and of 29.0% for the LDA algorithm without the MV application.
Hence, it is fair to say that the KNN resulted to be the best classification algorithm, capable to perform a good classification also without the use of the MV, which is instead necessary in the cases of the SVM or LDA for enhancing their performance. In a view of a real time application, the MV could be safely adopted in this contest because it showed the ability to easily classify in the correct way all the spurious elements especially in the KNN algorithm adopted, while with SVM and LDA the performances are not sufficient.
Another important aspect to note regards the features that are inside the five sets. After the analysis performed it's possible to obtain some information regarding the features that are characterised by the highest information content. The TDAR (MAV, SSC, WL, VAR, WAMP, AR, ZC) results to be the optimal feature set in terms of accuracy and precision. Considering instead the Hudgins set (MAV, WL, SSC, ZC), which is characterised by only time-domain features like the TDAR, for the purpose of this study it resulted to be not suitable in terms of information content, representing, on average, the worst feature set (60.8% of accuracy in the case of KNN without MV). A possible explanation could be that the three features (VAR, WAMP, AR) present in the TDAR set but not in the Hudgins set, were characterized by a high information content. The Du (IEMG, VAR, WAMP, WL, SSC, ZC) and the Phinyomark 2 (WPermEN, CC, RMS, WL) feature sets showed instead a comparable performance in terms of accuracy (65.4% and 69.2% respectively, in the best cases of KNN without MV), and they are still composed by only time-domain features. After that, it's required a focus to the good results obtained from the Phinyomark feature set 1 where there are five time-domain features and only two in the frequency domain, which likely add important informational content. This is confirmed by the p-values coming from the comparison among the accuracy values previously expressed.

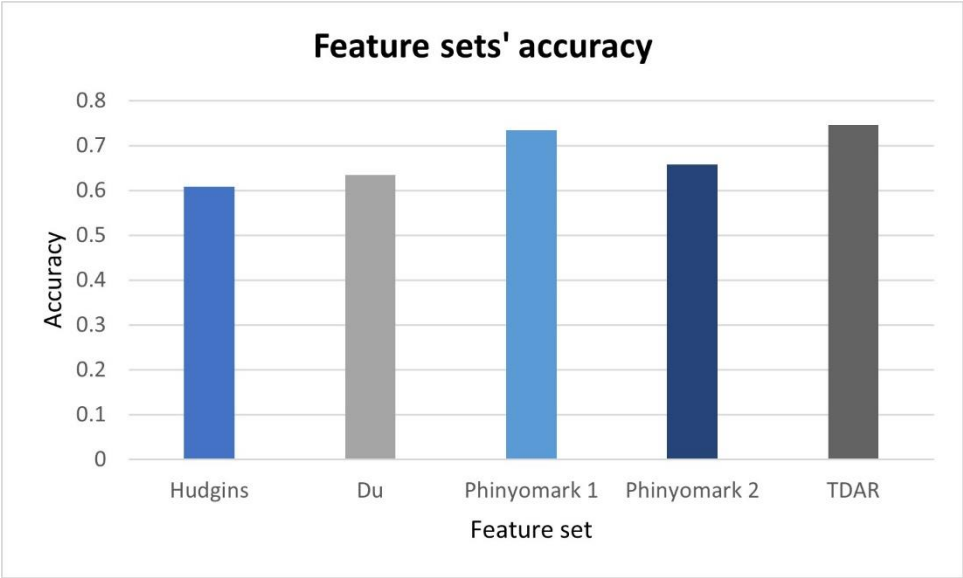

Figure 28: Bar plot of the accuracy regarding the KNN, respectively in all the five feature set before the majority voting was applied.

4.3 Effect of reduced electrodes setup over global performance

From only six electrodes it resulted possible to obtain a great amount of information needed, for distinguishing between 30 classes. Anyway, the last aspect investigated in this thesis is how much the reduction of the electrodes can influence the classification. The six electrodes initially considered have been divided in forearm electrodes and wrist electrodes. It's possible to say that also in this case the KNN algorithm showed the best results. The TDAR feature set confirms to be the most accurate feature set, followed by the Phinyomark 1, as shown in the section *3.2.1 Reduced electrodes setup*. More in detail, as reported in figure 29, the KNN accuracies from all the electrodes, the forearm and wrist are compared using the TDAR feature set. The statistical comparison between the all-electrodes setup (74.6% of accuracy) and the wrist setup (28.3% accuracy) highlighted that the wrist electrodes alone are not sufficient for having the correct amount on information ($p=0.0012$). Comparing with the forearm electrodes, (59.0% of accuracy) also in this case the information content is reduced with respect to all the electrodes considered, with a statistically significant difference in terms of accuracy ($p=0.0022$). The MV application provokes a rise of the only forearm electrodes accuracy to 84.8%, against all electrodes' accuracy of 94.0%, which means that in terms of real time application the use of only the four forearm electrodes can be suitable to obtain a reliable handwritten words recognition. This can be a good solution in case of amputee patients that can still give information by contracting the only forearm muscles and, in general, a low number of probes is always recommended in order

to have a less invasive and cumbersome recording setup. In contrast to gesture recognition problems, where it was shown in literature that few-electrodes setups are sufficient for a correct gesture classification [43], in handwriting recognition problem, due to due to complexity of the task, setups involving a relatively high number of probes are shown to be required [33] and this was confirmed by the present study.

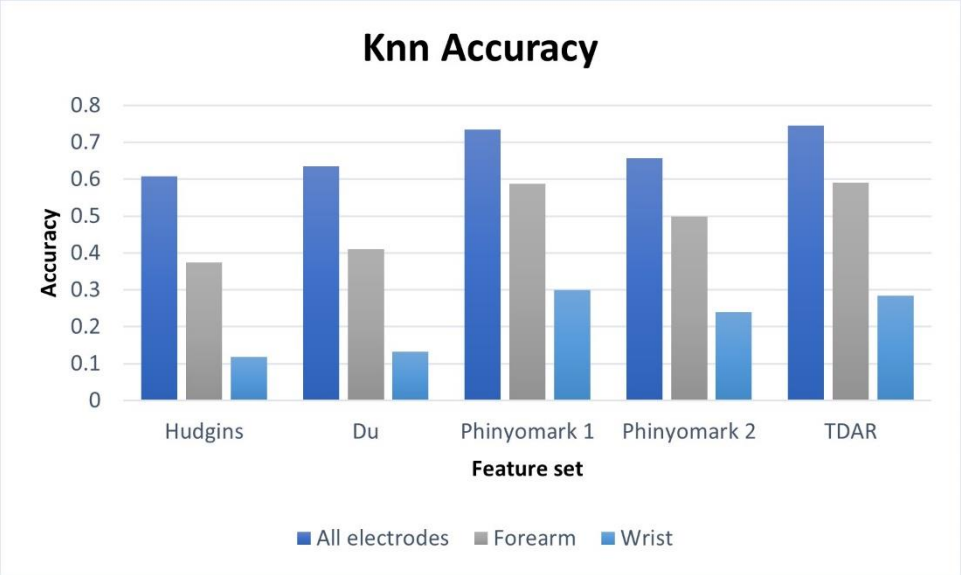

Figure 29: Bar plot of the accuracy regarding the KNN in the five feature sets, expressing the difference between the performance when all the electrodes (in blue), forearm (in grey) or wrist (in light blue) electrodes are considered (before majority voting application).

In conclusion it was showed that the myoelectric pattern recognition is a reliable method for performing handwriting recognition. In contrast to hand gesture recognition problems, due to the high complexity of the task, it was showed that when dealing with handwriting a spatial coverage of forearm and wrist with surface probes contemporaneously is essential to achieve the high classification accuracy, even if the only forearm information appeared to provide good results.

The comparison between three different classification algorithms (SVM, LDA and KNN) highlighted that the last one is the most appropriate in this pattern recognition problem, even if also the SVM gave quite good results, despite it is more expensive in terms of training time. Following that, the within subject analysis showed that the TDAR is the optimal feature set in terms of accuracy and precision, followed by the Phinyomark 1 feature sets, that includes features both in time and in frequency domain plus the autoregressive coefficients.

Further research may be devoted to the reduction of the feature sets dimensionality since it could be an important aspect for a faster computation. Another aspect could be the combination of different

handwriting recognition methods, like exploiting contemporaneously EMG data and kinematic data, for instance using accelerometer devices in conjunction with EMG electrodes or commercial armbands. Moreover, further research could focus on using other types of classifiers and expand the pattern recognition to complex sentences analysis, increasing even more the discriminating performance in myoelectric based handwriting recognition.

5 References

[1] Laura Dinehart, "Handwriting in early childhood education: Current research and future implications," *Journal of Early Childhood Literacy*, vol. 15, 2014.

[2] Samuel Planton, Mélanie Jucla, Franck-Emmanuel Roux, and Jean-François Démonet, "The 'handwriting brain': a meta-analysis of neuroimaging studies of motor versus orthographic processes.," *Cortex*, vol. 49(10), pp. 2772–2787, 2013.

[3] Marieke Longcamp, Jean-luc Velay, Virginia Wise Berninger, and Todd Richards., "Neuroanatomy of handwriting and related reading and writing skills in adults and children with and without learning disabilities: French-american connections.," *Pratiques. Linguistique, littérature, didactique*, pp. 171–172, 2016.

[4] Lambert Schomaker, "Handling within-writer variability and between-writer variation in the recognition of on-line handwriting.," *Citeseer*, 1995.

[5] Moussa Djioua and Réjean Plamondon, "Studying the variability of handwriting patterns using the kinematic theory," *Hum Mov Sci*, vol. 28(5), pp. 588–601, 2009.

[6] MONIKA Saini and A Kapoor, "Variability in handwriting patterns among ethnic groups of india," *International Journal of Humanities and Social Sciences*, vol. 2014b; 1 (3):49, p. 60, 2014.

[7] Charles C. Tappert, Ching Y. Suen, and Toru Wakahara, "The state of the art in online handwriting recognition," *IEEE Trans Pattern Anal Mach Intell*, vol. 12(8), pp. 787–808, 1990.

[8] G. D. Cascarano *et al.*, "Biometric handwriting analysis to support Parkinson's Disease assessment and grading," *BMC Med Inform Decis Mak*, vol. 19, no. 9, 2019, doi: 10.1186/s12911-019-0989-3.

[9] Charles C Tappert and Sung-Hyuk Cha, "English language handwriting recognition interface ," *Text entry systems: Mobility, accessibility, universality*, pp. 123–137, 2007.

[10] Rohini Salunke, Dipali Badhe, Vanita Doke, Yogeshwari Raykar, and Bhushan S Thakare., " The state of the art in text recognition techniques".

[11] Silvestro Micera, Jacopo Carpaneto, and Stanisa Raspopovic, "Control of hand prostheses using peripheral information ," *IEEE reviews in biomedical engineering*, vol. 3, pp. 48–68, 2010.

[12] J. Danna *et al.*, "Handwriting Movement Sonification for the Rehabilitation of Dysgraphia," 2013. [Online]. Available: https://hal.archives-ouvertes.fr/hal-00874974

[13] Jankovic J, "Parkinson's disease: clinical features and diagnosis," *J Neurol Neurosurg Psychiatry*, vol. 79(4), pp. 368–376, 2008.

[14] Wagle Shukla A, Ounpraseuth S, Okun MS, Gray V, Schwankhaus J, and Metzer WS., " Micrographia and related deficits in Parkinson's disease: a cross-sectional study," *BMJ Open*, vol. 2(3), 2012.

[15] A. Ziliotto, M. G. Cersosimo, and F. E. Micheli, "Handwriting rehabilitation in parkinson disease: A pilot study," *Ann Rehabil Med*, vol. 39, no. 4, pp. 586–591, 2015, doi: 10.5535/arm.2015.39.4.586.

[16] E. Nackaerts *et al.*, "Handwriting training in Parkinson's disease: A trade-off between size, speed and fluency," *PLoS One*, vol. 12, no. 12, Dec. 2017, doi: 10.1371/journal.pone.0190223.

[17] H. S. R. Kao, S. P. W. Lam, and T. T. Kao, "Chinese calligraphy handwriting (CCH): A case of rehabilitative awakening of a coma patient after stroke," *Neuropsychiatr Dis Treat*, vol. 14, pp. 407–417, Jan. 2018, doi: 10.2147/NDT.S147753.

[18] H. S. R. Kao, "Calligraphy therapy: A complementary approach to psychotherapy," *Asia Pac J Couns Psychother*, vol. 1, no. 1, pp. 55–66, Feb. 2010, doi: 10.1080/21507680903570334.

[19] M. Pąchalska, M. Moskała, B. Duncan MacQueen, J. Polak, and M. Wilk-Frańczuk, "Early neurorehabilitation in a patient with severe traumatic brain injury to the frontal lobes."

[20] M. Asghari Oskoei and H. Hu, "Myoelectric control systems-A survey," *Biomedical Signal Processing and Control*, vol. 2, no. 4. Elsevier BV, pp. 275–294, 2007. doi: 10.1016/j.bspc.2007.07.009.

[21] S. Micera, J. Carpaneto, and S. Raspopovic, "Control of hand prostheses using peripheral information," *IEEE Rev Biomed Eng*, vol. 3, pp. 48–68, 2010, doi: 10.1109/RBME.2010.2085429.

[22] K. Englehart and B. Hudgins, "A Robust, Real-Time Control Scheme for Multifunction Myoelectric Control," *IEEE Trans Biomed Eng*, vol. 50, no. 7, pp. 848–854, 2003, doi: 10.1109/TBME.2003.813539.

[23] A. H. Al-Timemy, G. Bugmann, J. Escudero, and N. Outram, "Classification of finger movements for the dexterous hand prosthesis control with surface electromyography," *IEEE J Biomed Health Inform*, vol. 17, no. 3, pp. 608–618, 2013, doi: 10.1109/JBHI.2013.2249590.

[24] A. Phinyomark, F. Quaine, S. Charbonnier, C. Serviere, F. Tarpin-Bernard, and Y. Laurillau, "EMG feature evaluation for improving myoelectric pattern recognition robustness," *Expert Syst Appl*, vol. 40, no. 12, pp. 4832–4840, 2013, doi: 10.1016/j.eswa.2013.02.023.

[25] N. Parajuli *et al.*, "Real-time EMG based pattern recognition control for hand prostheses: A review on existing methods, challenges and future implementation," *Sensors (Switzerland)*, vol. 19, no. 20. MDPI AG, Oct. 02, 2019. doi: 10.3390/s19204596.

[26] X. Li, O. W. Samuel, X. Zhang, H. Wang, P. Fang, and G. Li, “A motion-classification strategy based on sEMG-EEG signal combination for upper-limb amputees,” *J Neuroeng Rehabil*, vol. 14, no. 1, pp. 1–13, Jan. 2017, doi: 10.1186/s12984-016-0212-z.

[27] D. Bai, S. Chen, and J. Yang, “Upper Arm Motion High-Density sEMG Recognition Optimization Based on Spatial and Time-Frequency Domain Features,” *J Healthc Eng*, vol. 2019, 2019, doi: 10.1155/2019/3958029.

[28] L. H. Smith, L. J. Hargrove, B. A. Lock, and T. A. Kuiken, “Determining the optimal window length for pattern recognition-based myoelectric control: Balancing the competing effects of classification error and controller delay,” *IEEE Transactions on Neural Systems and Rehabilitation Engineering*, vol. 19, no. 2, pp. 186–192, Apr. 2011, doi: 10.1109/TNSRE.2010.2100828.

[29] N. E. Bunderson and T. A. Kuiken, “Quantification of feature space changes with experience during electromyogram pattern recognition control,” *IEEE Transactions on Neural Systems and Rehabilitation Engineering*, vol. 20, no. 3, pp. 239–246, 2012, doi: 10.1109/TNSRE.2011.2182525.

[30] R. C. de Freitas, G. R. Naik, M. J. S. Valença, B. L. D. Bezerra, R. E. de Souza, and W. P. dos Santos, “Surface electromyography classification using extreme learning machines and echo state networks,” *Research on Biomedical Engineering*, vol. 38, no. 2, pp. 477–498, Jun. 2022, doi: 10.1007/s42600-022-00201-7.

[31] Khushaba RN, Kodagoda S, Takruri M, and Dissanayake G, “Toward improved control of prosthetic fingers using surface electromyogram (emg) signals,” *Expert Syst Appl.* , vol. 39(12), pp. 10731–10738, 2012.

[32] E. Okorokova, M. Lebedev, M. Linderman, and A. Ossadtchi, “A dynamical model improves reconstruction of handwriting from multichannel electromyographic recordings,” *Front Neurosci*, vol. 9, no. OCT, 2015, doi: 10.3389/fnins.2015.00389.

[33] M. Linderman, M. A. Lebedev, and J. S. Erlichman, “Recognition of handwriting from electromyography,” *PLoS One*, vol. 4, no. 8, Aug. 2009, doi: 10.1371/journal.pone.0006791.

[34] P. H. T. Q. de Almeida, D. M. C. da Cruz, L. A. Magna, and I. S. V. Ferrigno, “An electromyographic analysis of two handwriting grasp patterns,” *Journal of Electromyography and Kinesiology*, vol. 23, no. 4, pp. 838–843, Aug. 2013, doi: 10.1016/j.jelekin.2013.04.004.

[35] Z. Yang and Y. Chen, “Surface EMG-based sketching recognition using two analysis windows and gene expression programming,” *Front Neurosci*, vol. 10, no. OCT, Oct. 2016, doi: 10.3389/fnins.2016.00445.

[36] Y. Chen and Z. Yang, “A novel hybrid model for drawing trace reconstruction from multichannel surface electromyographic activity,” *Front Neurosci*, vol. 11, no. FEB, Feb. 2017, doi: 10.3389/fnins.2017.00061.

[37] J. G. Beltran-Hernandez, J. Ruiz-Pinales, P. Lopez-Rodriguez, J. L. Lopez-Ramirez, and J. G. Avina-Cervantes, “Multi-Stroke handwriting character recognition based on sEMG using convolutional-recurrent neural networks,” *Mathematical Biosciences and Engineering*, vol. 17, no. 5, pp. 5432–5448, Aug. 2020, doi: 10.3934/MBE.2020293.

[38] Alan M Wing, “variability in handwritten characters,” *Visible Lang*, vol. 13(3), pp. 283–298, 1979.

[39] C. J. de Luca, “Physiology and Mathematics of Myoelectric Signals,” *IEEE Trans Biomed Eng*, vol. BME-26, no. 6, pp. 313–325, 1979, doi: 10.1109/TBME.1979.326534.

[40] P. Konrad, “The abc of emg.” [Online]. Available: https://www.researchgate.net/publication/270895853

[41] L. Ricardo, J. Luiz, M. Bigliassi, T. F. Dias Kanthack, A. C. de Moraes, and T. Abrao, “Influence of Different Strategies of Treatment Muscle Contraction and Relaxation Phases on EMG Signal Processing and Analysis During Cyclic Exercise,” in *Computational Intelligence in Electromyography Analysis - A Perspective on Current Applications and Future Challenges*, InTech, 2012. doi: 10.5772/50599.

[42] Weiting Chen, Zhizhong Wang, Hongbo Xie, and Wangxin Yu, “Characterization of surface emg signal based on fuzzy entropy,” *IEEE Transactions on neural systems and rehabilitation engineering*, vol. 15(2), pp. 266–272, 2007.

[43] F. S. Botros, A. Phinyomark, and E. J. Scheme, “Electromyography-Based Gesture Recognition: Is It Time to Change Focus from the Forearm to the Wrist?,” *IEEE Trans Industr Inform*, vol. 18, no. 1, pp. 174–184, Jan. 2022, doi: 10.1109/TII.2020.3041618.

[44] E. van Oudenaarde’ And and R. A. B. Oostendorp2, “Functional relationship between the abductor pollicis longus and abductor pollicis brevis muscles: an EMG analysis,” 1995.

[45] Martin Petkov, “The elbow: joint structure, movements and muscles. https://www.martinpetkov.com/your-opportunity/the-elbow-joint-structure-movements-and-muscles,” 2013.

[46] Ambrosi Glauco et Al., “ANATOMIA DELL’UOMO,” pp. 131–142, 2008.

[47] Oliver Jones, “Muscles of the Upper Limb, https://teachmeanatomy.info,” *TeachMe Anatomy*, 2020.

[48] “https://web.archive.org/web/20111226085859/http://oxforddictionaries.com/words/the-oec-facts-about-the-language.”

[49] J. Huang, “A common construction pattern of English words and Chinese characters.,” *PLoS One*, vol. 8, no. 9, 2013, doi: 10.1371/journal.pone.0074515.

[50] HJA Van Hedel, L Tomatis, and R Müller, “Modulation of leg muscle activity and gait kinematics by walking speed and bodyweight unloading,” *Gait Posture*, vol. 24(1), pp. 35–45, 2006.

[51] Lars Arendt-Nielsen, Thomas Graven-Nielsen, Heine Svarrer, and Peter Svensson, “The influence of low back pain on muscle activity and coordination during gait: a clinical and experimental study,” *Pain*, vol. 64(2), pp. 231–240, 1996.

[52] Asad Ullah, Sarwan Ali, Imdadullah Khan, Muhammad Asad Khan, and Safiullah Faizullah., “ Effect of analysis window and feature selection on classification of hand movements using emg signal,” *In Proceedings of SAI Intelligent Systems Conference*, pp. 400–415, 2020.

[53] Oluwarotimi Williams Samuel *et al.*, “ Intelligent emg pattern recognition control method for upper-limb multifunctional prostheses: advances, current challenges, and future prospects,” *Ieee Access*, vol. 7, pp. 10150–10165, 2019.

[54] Erik Scheme and Kevin Englehart, “Electromyogram pattern recognition for control of powered upper-limb prostheses: state of the art and challenges for clinical use.,” *J Rehabil Res Dev*, vol. 48(6), 2011.

[55] Todd R Farrell and Richard F Weir, “The optimal controller delay for myoelectric prostheses.,” *IEEE Transactions on neural systems and rehabilitation engineering*, vol. 15(1), pp. 111–118, 2007.

[56] A. Phinyomark, F. Quaine, S. Charbonnier, C. Serviere, F. Tarpin-Bernard, and Y. Laurillau, “EM G Feature Evaluation for I mproving M yoelectric Pattern Recognition Robustness.”

[57] S. Fioretti, F. Barbarossa, A. Mengarelli, A. Tigrini, “UNIVERSITÀ POLITECNICA DELLE MARCHE FACOLTÀ DI INGEGNERIA Handwriting Characterization: a Myoelectric-based Pattern Recognition Approach.”

[58] Hiroshi Tanaka, Naomi Iwayama, and Katsuhiko Akiyama, “Online handwriting recognition technology and its applications ,” *FUJITSU Sci. Tech. J*, vol. 40(1), pp. 170–178, 2004.

[59] Angkoon Phinyomark, Pornchai Phukpattaranont, and Chusak Limsakul., “ Feature reduction and selection for emg signal classification ,” *Expert Syst Appl*, vol. 39(8), pp. 7420–7431, 2012.

[60] M. , W. B. C. , B. K. , &Hashemi, R. M. Zardoshti-Kermani, “EMG feature evaluation for movement control ofupper extremity prostheses,” *IEEE Transactions on Rehabilitation Engineering*, vol. 3(4), pp. 324–333, 1995.

[61] D. , Tkach, H. , Huang, and T. A. Kuiken, “Study ofstability oftime-domain features for electromyographic pattern recognition.,” *Journal of NeuroEngineering and Rehabilitation*, vol. 7(21), 2010.

[62] Bilal Fadlallah, Badong Chen, Andreas Keil, and Jose Principe, “Weighted-permutation entropy: A complexity measure for time series incorporating amplitude information,” *Phys Rev E*, vol. 87(2):022911, 2013.

[63] Dario Farina and Roberto Merletti, “Comparison of algorithms for estimation of emg variables during voluntary isometric contractions. ,” *Journal of Electromyography and Kinesiology*, vol. 10(5), pp. 337–349, 2000.

[64] Sijiang Du and Marko Vuskovic, “Temporal vs. spectral approach to feature extraction from prehensile emg signals,” *n Proceedings of the 2004 IEEE International Conference on Information Reuse and Integration*, pp. 344–350, 2004.

[65] D. Moshou, I. Hostens, G. Papaioannou, and H. Ramon, “WAVELETS AND SELF-ORGANISING MAPS IN ELECTROMYOGRAM (EMG) ANALYSIS.”

[66] TM Inbamalar and R Sivakumar, “Improved algorithm for analysis of dna sequences using multiresolution transformation. ,” *The Scientific World Journal*, 2015.

[67] C. S. Park, J. H. Choi, S. P. Nah, W. Jang, and D. Y. Kim, “Automatic modulation recognition of digital signals using wavelet features and SVM,” in *International Conference on Advanced Communication Technology, ICACT*, 2008, vol. 1, pp. 387–390. doi: 10.1109/ICACT.2008.4493784.

[68] B. Hudgins, P. Parker, and R. N. Scott, “A New Strategy for Multifunction Myoelectric Control,” *IEEE Trans Biomed Eng*, vol. 40, no. 1, pp. 82–94, 1993, doi: 10.1109/10.204774.

[69] Yi-Chun Du, Chia-Hung Lin, Liang-Yu Shyu, and Tainsong Chen, “Portable hand motion classifier for multi-channel surface electromyography recognition using grey relational analysis.,” *Expert Systems with Applications*, vol. 37(6), pp. 4283–4291, 2010.

[70] H. Huang, H. B. Xie, J. Y. Guo, and H. J. Chen, “Ant colony optimization-based feature selection method for surface electromyography signals classification,” *Comput Biol Med*, vol. 42, no. 1, pp. 30–38, Jan. 2012, doi: 10.1016/j.compbiomed.2011.10.004.

[71] K. Englehart, B. Hudgins, and P. A. Parker, “A wavelet-based continuous classification scheme for multifunction myoelectric control,” *IEEE Trans Biomed Eng*, vol. 48, no. 3, pp. 302–311, 2001, doi: 10.1109/10.914793.

[72] Jason Brownlee., “ Linear discriminant analysis for machine learning,” *Machine learning mastery,* , vol. 6, 2016.

[73] B. Farnham, S. Tokyo, B. Boston, F. Sebastopol, and T. Beijing, “Hands-on Machine Learning with Scikit-Learn, Keras, and TensorFlow Concepts, Tools, and Techniques to Build Intelligent Systems SECOND EDITION.”

[74] S. Ding, J. Yu, B. Qi, and H. Huang, “An overview on twin support vector machines,” *Artif Intell Rev*, vol. 42, no. 2, pp. 245–252, 2014, doi: 10.1007/s10462-012-9336-0.

[75] Alexandre KOWALCZYK, “SVM - Understanding the math - the optimal hyperplane, https://www.svm-tutorial.com/2015/06/svm-understanding-math-part-3/,” *SVM Tutorial*, Jun. 08, 2015.

[76] MathWorks, “Support Vector Machine (SVM),Impara a usare gli iperpiani ottimali come confini decisionali, https://it.mathworks.com/discovery/support-vector-machine.html,” *MathWorks*.

[77] A. R. Lubis, M. Lubis, and Al-Khowarizmi, “Optimization of distance formula in k-nearest neighbor method,” *Bulletin of Electrical Engineering and Informatics*, vol. 9, no. 1, pp. 326–338, Feb. 2020, doi: 10.11591/eei.v9i1.1464.

[78] N. Krisandi, et al. “The k-nearest neighbor algorithm in the classification of palm oil production data at PT. Minamas, Parindu sub-district ,” *Bimaster*, vol. 2(1), 2013.

[79] X. Pan, et al “K-nearest neighbor based structural twin support vector machine,” *Knowl Based Syst*, vol. 88, pp. 34–44, 2015.

[80] Haji Samadi and Mohammad Reza, “ Eye Tracking with EEG life-style ,” 2015.

[81] D. Chicco and G. Jurman, “The advantages of the Matthews correlation coefficient (MCC) over F1 score and accuracy in binary classification evaluation. .,” *BMC Genomics 21*, vol. 6, 2020.

[82] A. Aras, “Explaining what learned models predict: In which cases can we trust machine learning models and when is caution required ?,” *BOOK*, 2020.

[83] Y. Huang, K. B. Englehart, B. Hudgins, and A. D. C. Chan, “‘A Gaussian mixture model based classification scheme for myoelectric control of powered upper limb prostheses,’ ,” *IEEE Trans. Biomed. Eng.*, vol. 52(11), pp. 1801–1811, 2005.

[84] T. R. Farrell, “ ‘Determining delay created by multifunctional prosthesis controllers,’ ,” *J. Rehabil. Res. Develop.*, vol. 48(6), pp. 21–38, 2011.

[85] J. He, X. Sheng, X. Zhu, and N. Jiang, “Position Identification for Robust Myoelectric Control against Electrode Shift,” *IEEE Transactions on Neural Systems and Rehabilitation Engineering*, vol. 28, no. 12, pp. 3121–3128, Dec. 2020, doi: 10.1109/TNSRE.2020.3038374.

[86] M. F. Wahid, R. Tafreshi, and R. Langari, “A Multi-Window Majority Voting Strategy to Improve Hand Gesture Recognition Accuracies Using Electromyography Signal,” *IEEE Transactions on Neural Systems and Rehabilitation Engineering*, vol. 28, no. 2, pp. 427–436, Feb. 2020, doi: 10.1109/TNSRE.2019.2961706.

[87] R. N. Khushaba, "Correlation Analysis of Electromyogram Signals for Multiuser Myoelectric Interfaces," *IEEE Transactions on Neural Systems and Rehabilitation Engineering,* vol. 22, no. 4, pp. 745-755, July 2014.

[88] Rami N. Khushaba, Sarath Kodagoda, Maen Takruri, Gamini Dissanayake, "Toward improved control of prosthetic fingers using surface electromyogram (EMG) signals", *Expert Systems with Applications*, Volume 39, Issue 12, 2012.

[89] Chan ADC and Green GC, "'Myoelectric control development toolbox,'" *30th Conference of the Canadian Medical & Biological Engineering Society, Toronto, Canada, M0100*, 2007.

[90] Gibbons, J. D., and S. Chakraborti. Nonparametric Statistical Inference, 5th Ed., Boca Raton, FL: Chapman & Hall/CRC Press, Taylor & Francis Group, 2011.

[91] Hollander, M., and D. A. Wolfe. Nonparametric Statistical Methods. Hoboken, NJ: John Wiley & Sons, Inc., 1999.